# X-ray Spectral Diagnostics of the Physical Environment in Seyfert Galaxies and Galactic Black Hole Binaries

Ken EBISAWA

(ISAS/JAXA)

with H. Inoue, M. Tsujimoto, T. Miyakawa, N. Iso, H. Sameshima, M. Mizumoto, H. Yamasaki and E. Kusunoki

# Contents

# Contents

# 1.Introduction
# Broad iron features in AGNs

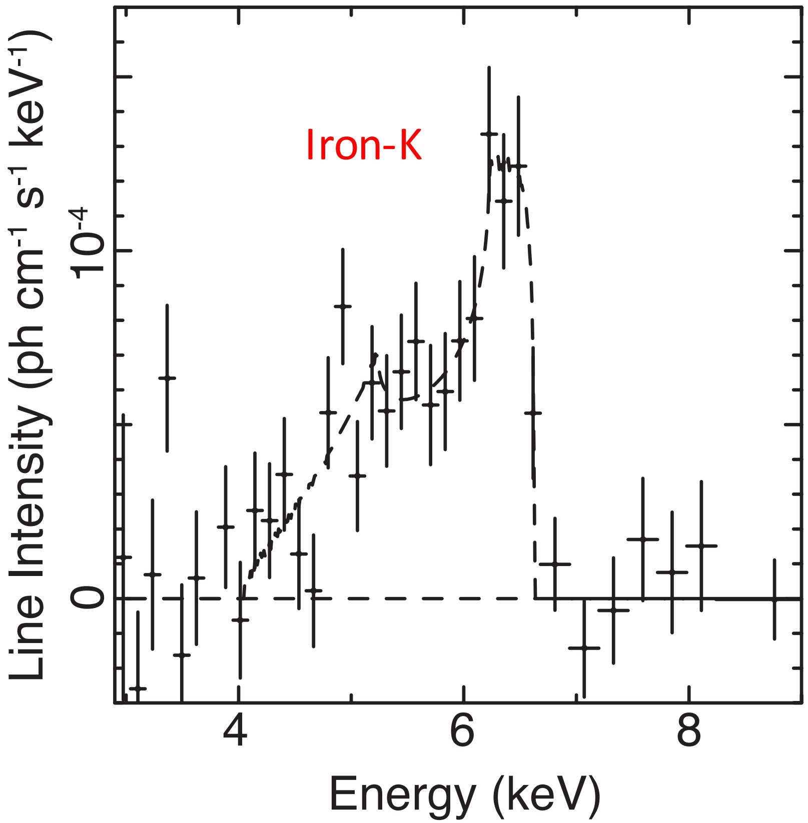


MCG-6-30-15 with ASCA (Tanaka+ 1995)

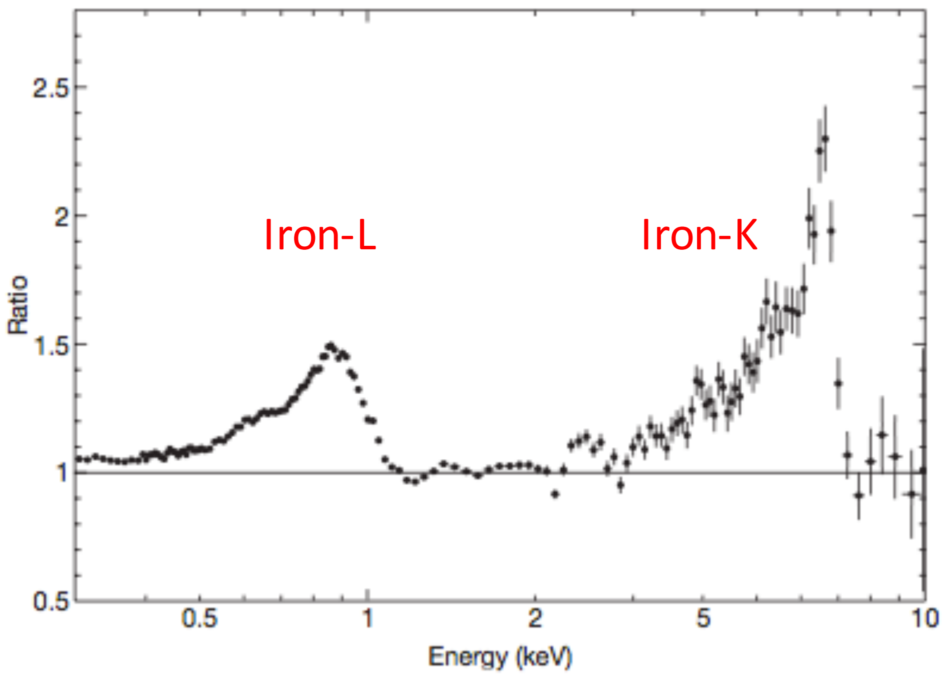


1H0707-495 with XMM (Fabian+ 2009)

- Look like broad Iron K- and L- emission lines

# 1.Introduction
# Broad iron features in BHBs

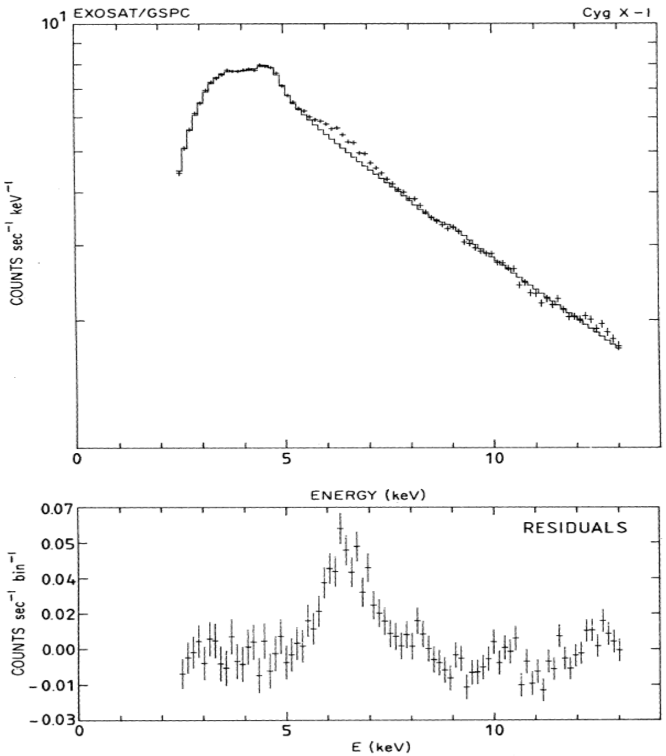


Cyg X-1 with EXOSAT
(Barr, White and Page 1985)

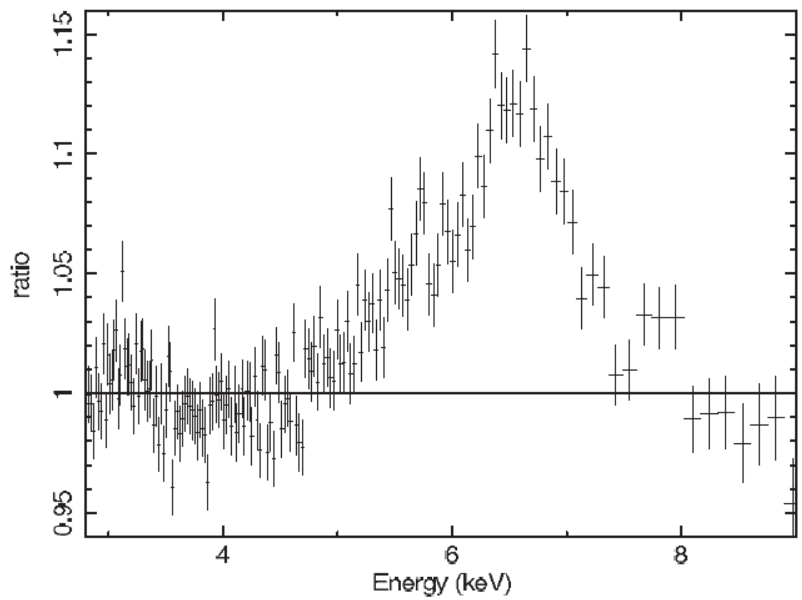


GRS1915+105 with Suzaku
(Blum et al. 2009)

- Broad Iron emission line features also observed from BHBs
- Presumably, they have the same origin as in AGNs

# Characteristic spectral variation in AGN

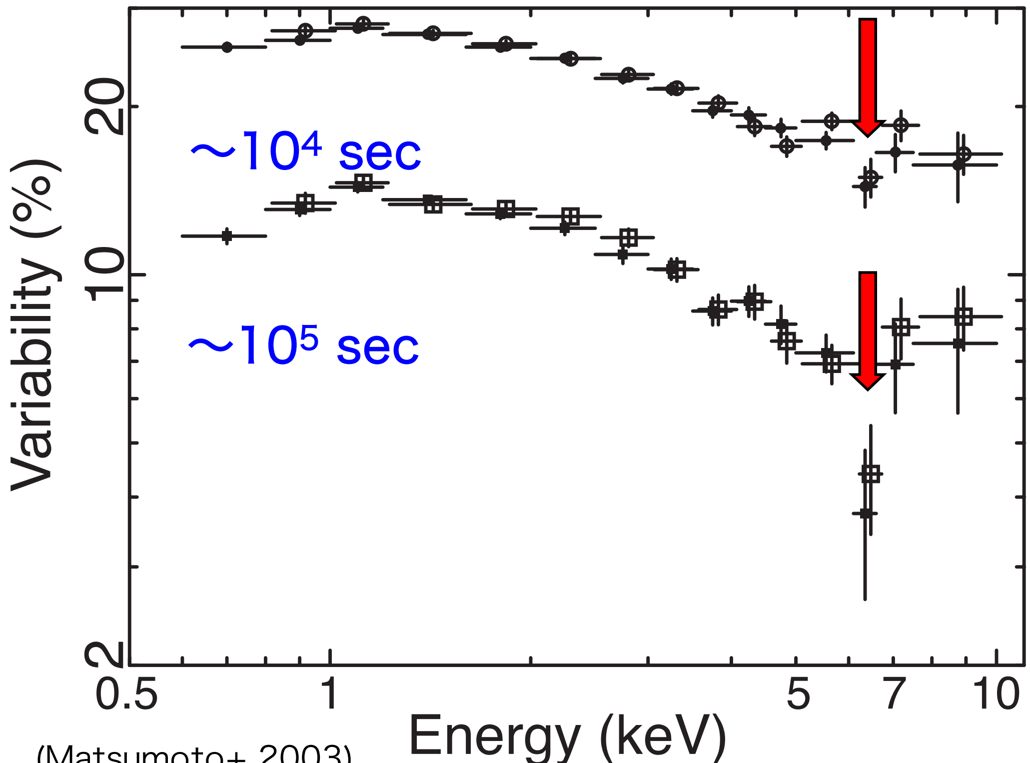

(Matsumoto+ 2003)

- MCG-6-30-15 with ASCA
  Energy dependence of the Root Mean Square varation (RMS spectra)
- Significant drop in the RMS spectra at the iron K-band
- Model independent result to be explained

- Two remarkable observational features
  - Seemingly broad iron K- and L-line features
  - Significant drop of RMS at iron K-line energy in AGN
- Strong diagnostics for physical environments around super-massive and/or stellar black holes

# Two competing models

1. Relativistic disk-line model
2. Partial covering model

# Relativistic disk-line model

- Miniutti and Fabian (2004)
  - Accretion disk is illuminated from above by a compact "lump-post" in the very vicinity (~Rs) of the black hole
  - The line is relativistically broadened ("disk-line")
  - Direct X-rays varies, while the reflection component does not very due to the relativistic "light-bending effect"

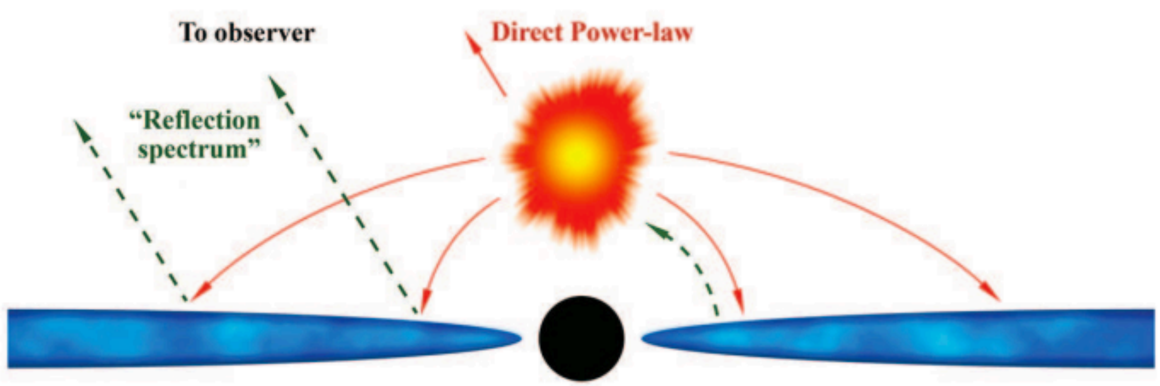


Fabian, Kara and Parker (2014)

# Partial Covering Model

- X-ray emission region is partially covered by intervening absorbers (e.g., Matsuoka+ 1990; McKernan and Yaqoob 1998; Miller, Turner and Reeves 2008, 2009)
- The RMS explained by variation of warm absorbers (Inoue and Matsumoto 2003)

# Two spectral models are degenerate

1. Relativistic disk-line model

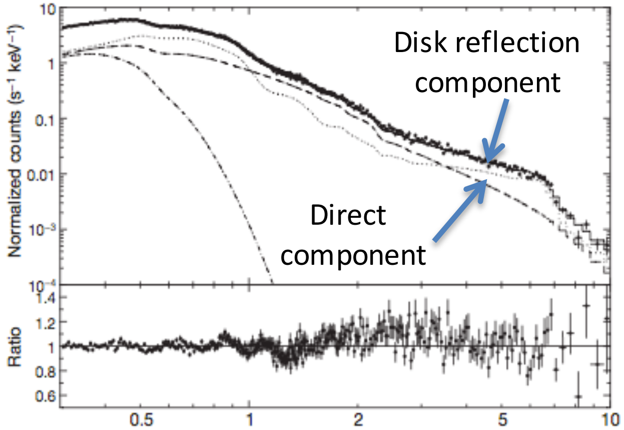


1H0707-495 with XMM (Fabian+ 2009)

X-ray emission region is required to be very compact (~Rs) so that the relativistic disk reflection takes place

2. Partial covering model

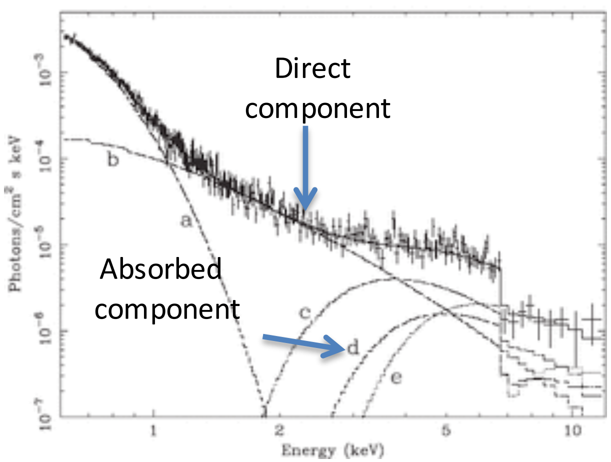


1H0707-495 with XMM (Tanaka+ 2004)

Partial covering clouds with a size of ~several Rs at a radius of ~100 Rs

The same X-ray spectra can be fitted by very different models

# Contents

# Contents

# Recently, evidence of the partial covering in AGN being accumulated

- Ursini et al. (2015), NGC5548

reflected component that is likely due to neutral material at least a few light months away from the continuum source. We confirm the presence of strong, partial covering X-ray absorption as the explanation for the sharp decrease in flux through the soft X-ray band.

- Parker, Walton, Fabian and Risaliti (2014), NGC1365

. As the variability in NGC 1365 is known to be due to changes in the parameters of a partial covering neutral absorber,
n shows relatively low absorption we separate the effects of intrinsic source variability, including signatures of relativisti

- Pounds (2014), PG1211+143

broad-band modelling indicated the need for a second, partial covering absorber to account for continuum curvature and spectral variability.

etc, etc…

- Variable Double Partial Covering Model (Miyakawa, Ebisawa and Inoue 2012)
  - Absorbers have internal ionization structures
  - Intrinsic X-ray luminosity from the AGN does not vary significantly in 1- 10 keV in timescales less than ~day
  - Most observed X-ray spectral variation (< day) below ~10 keV is explained by change of the partial covering fraction

# Variable Double Partial Covering (VDPC) Model

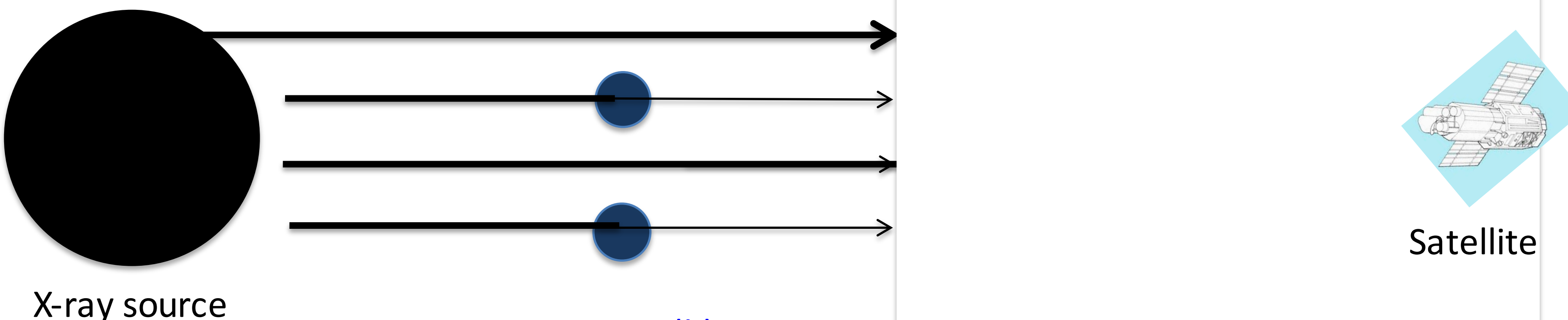


$( 1- \alpha+ \alpha\, \exp(-N_H^{(k)}\sigma(\xi_k))$ $))$

Partial covering by thick and cold absorbers with the partial covering fraction $\alpha$

Responsible for iron K-edge

Responsible for iron L-edge

# Variable Double Partial Covering (VDPC) Model

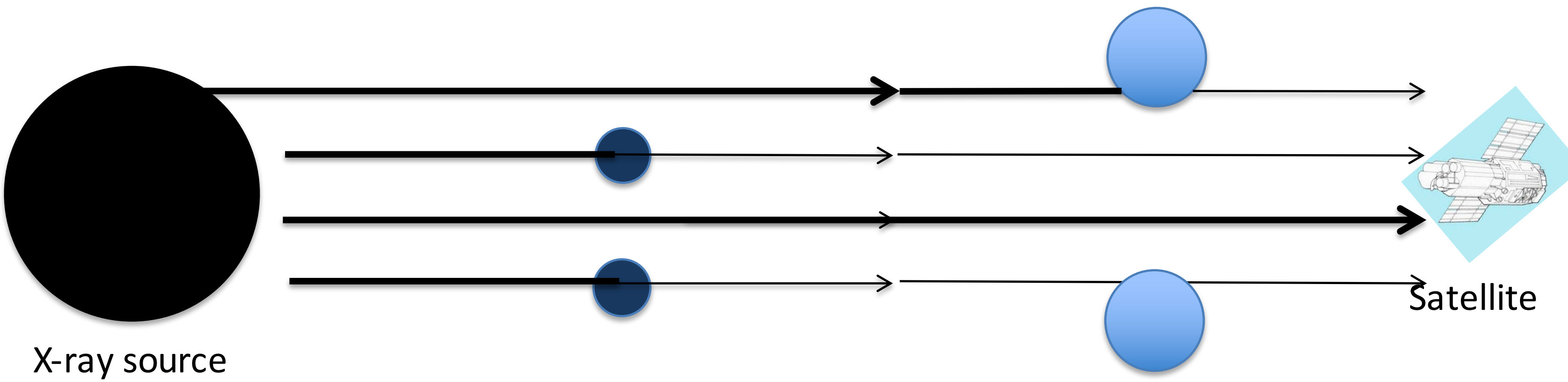

# Variable Double Partial Covering (VDPC) Model

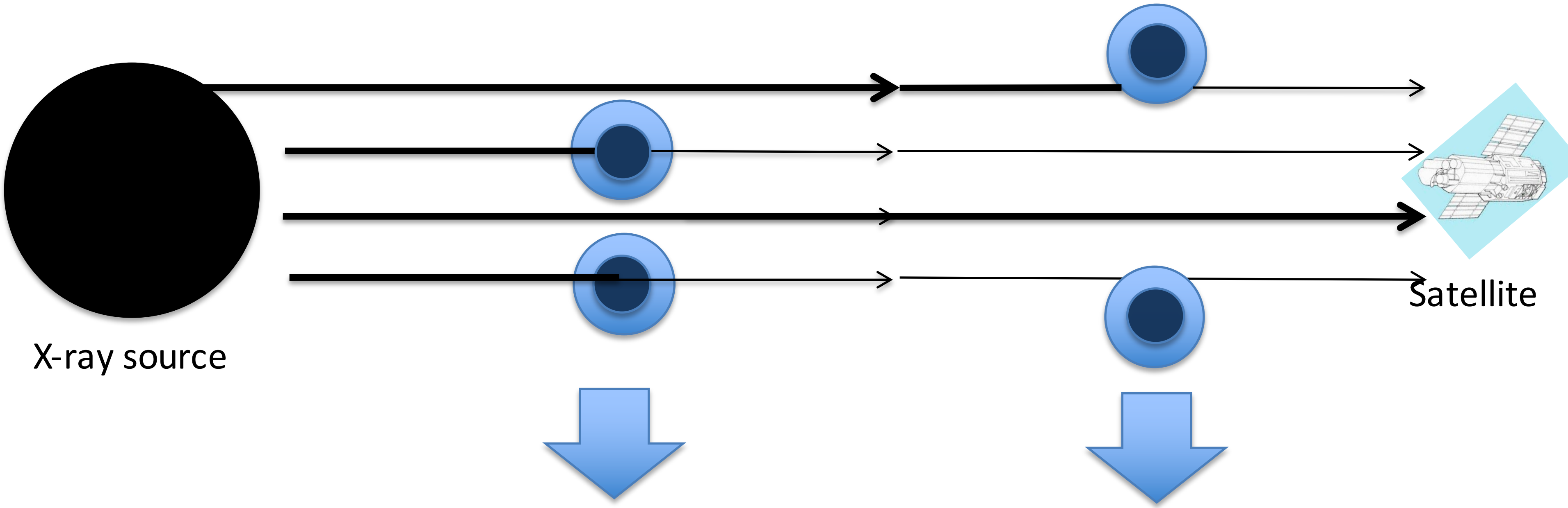


Thick and cold core responsible for the iron K-edge

Thin and hot envelope responsible for the iron L-edge

Presumably, the partial absorbers have inner structures; thick and cold core and thin and hot envelope

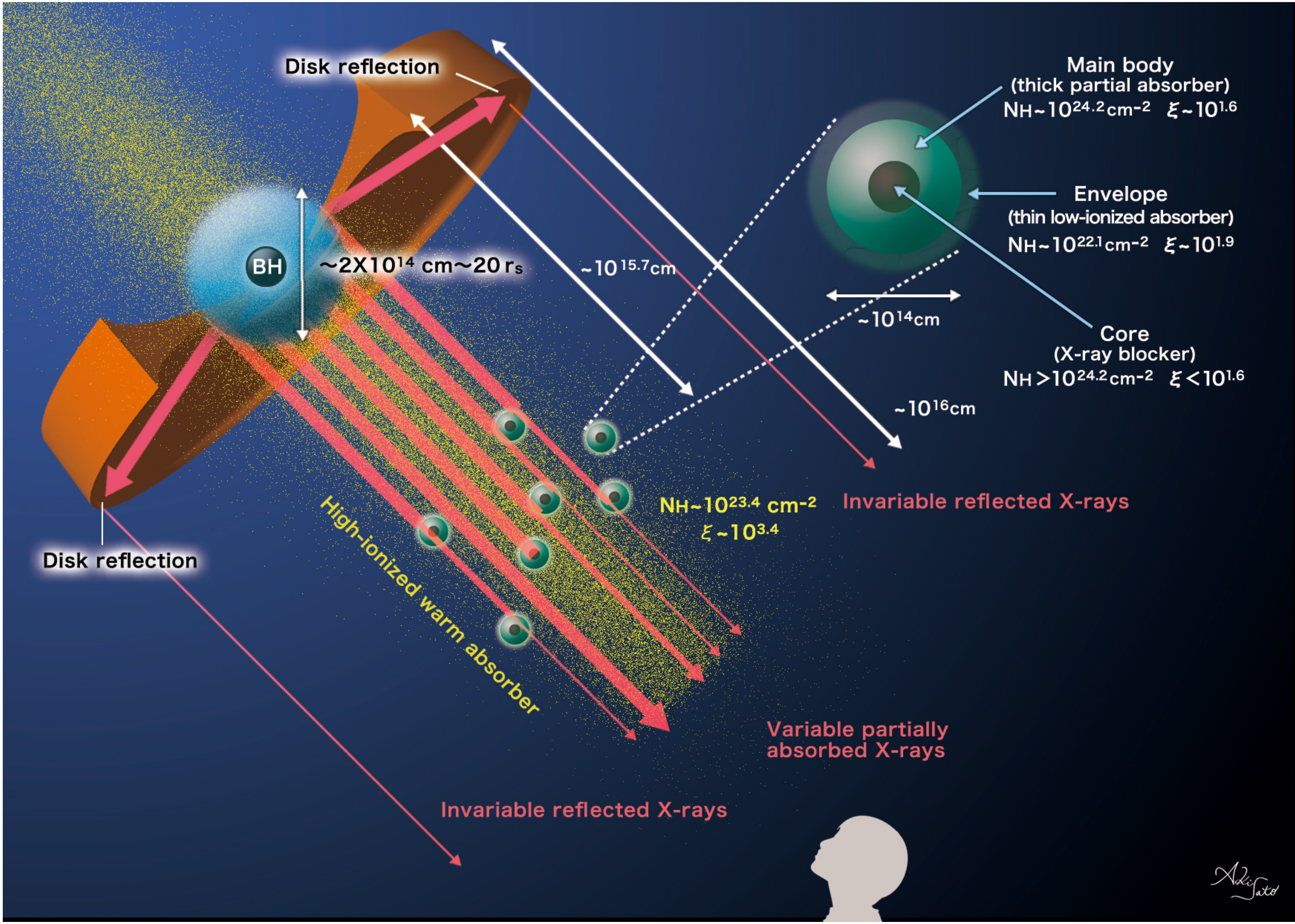


Miyakawa, Ebisawa and Inoue (2012)

# Variable Double Partial Covering Model

AGN luminosity and spectra below ~10 keV do not vary significantly within ~a day. Variation of the *partial covering fraction* explain most of the observed spectral variations below ~10 keV.

# Variable Double Partial Covering Model

AGN luminosity and spectra below ~10 keV do not vary significantly within ~a day. Variation of the *partial covering fraction* explain most of the observed spectral variations below ~10 keV.

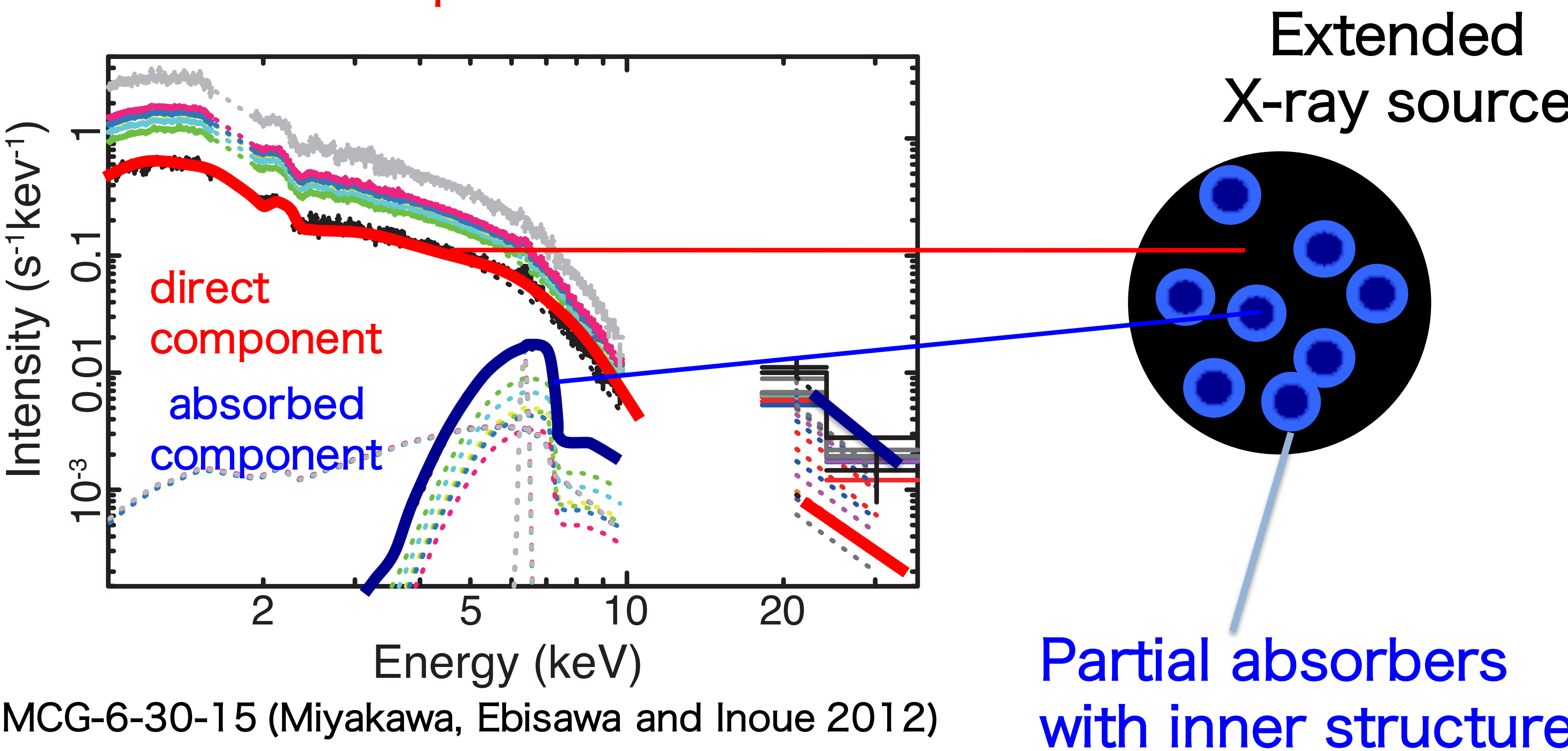


MCG-6-30-15 (Miyakawa, Ebisawa and Inoue 2012)

# Variable Double Partial Covering Model

AGN luminosity and spectra below ~10 keV do not vary significantly within ~a day. Variation of the *partial covering fraction* explain most of the observed spectral variations below ~10 keV.

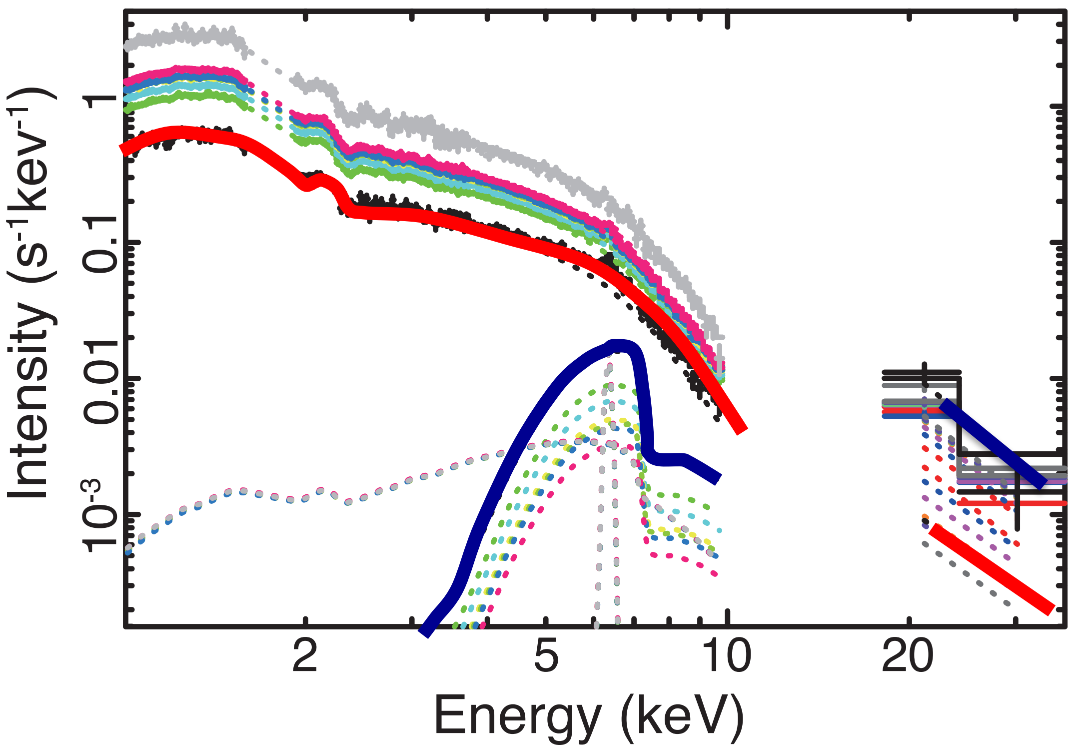


MCG-6-30-15 (Miyakawa, Ebisawa and Inoue 2012)

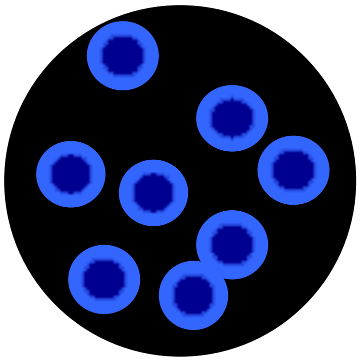

Covering fraction varies

# Variable Double Partial Covering Model

AGN luminosity and spectra below ~10 keV do not vary significantly within ~a day. Variation of the *partial covering fraction* explain most of the observed spectral variations below ~10 keV.

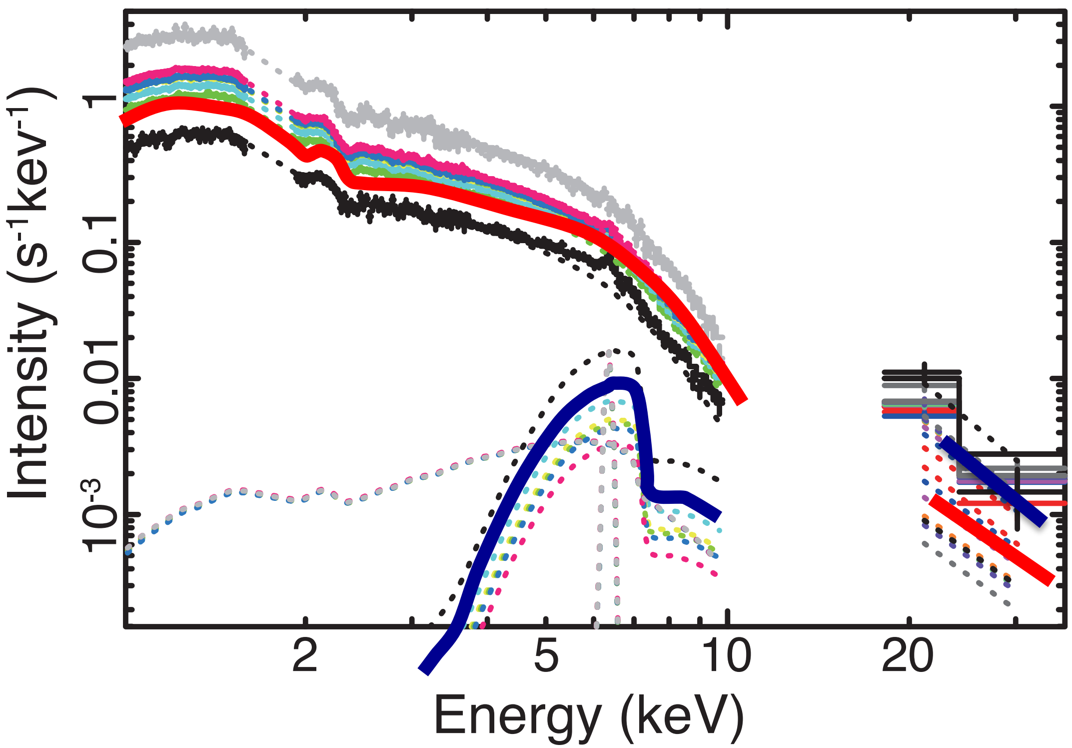


MCG-6-30-15 (Miyakawa, Ebisawa and Inoue 2012)

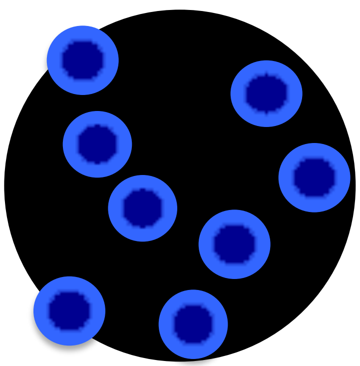

Covering fraction varies

# Variable Double Partial Covering Model

AGN luminosity and spectra below ~10 keV do not vary significantly within ~a day. Variation of the *partial covering fraction* explain most of the observed spectral variations below ~10 keV.

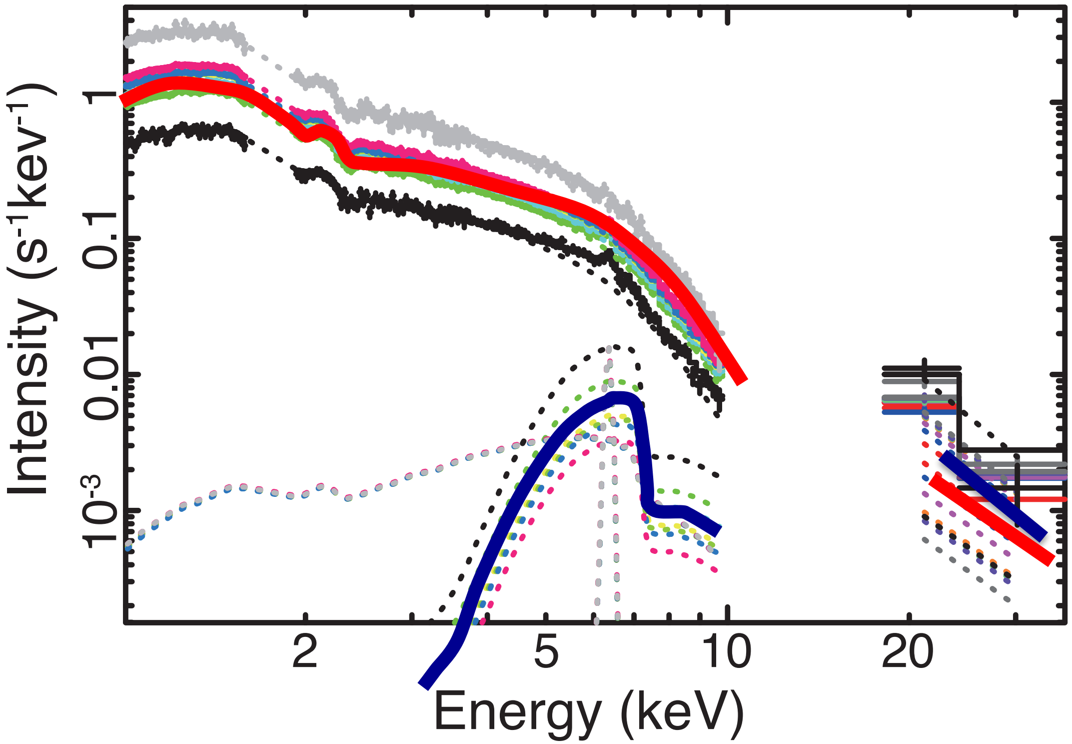


MCG-6-30-15 (Miyakawa, Ebisawa and Inoue 2012)

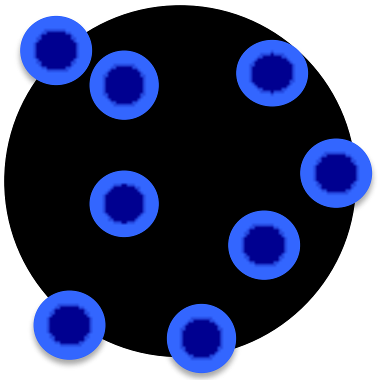

Covering fraction varies

# Variable Double Partial Covering Model

AGN luminosity and spectra below ~10 keV do not vary significantly within ~a day. Variation of the *partial covering fraction* explain most of the observed spectral variations below ~10 keV.

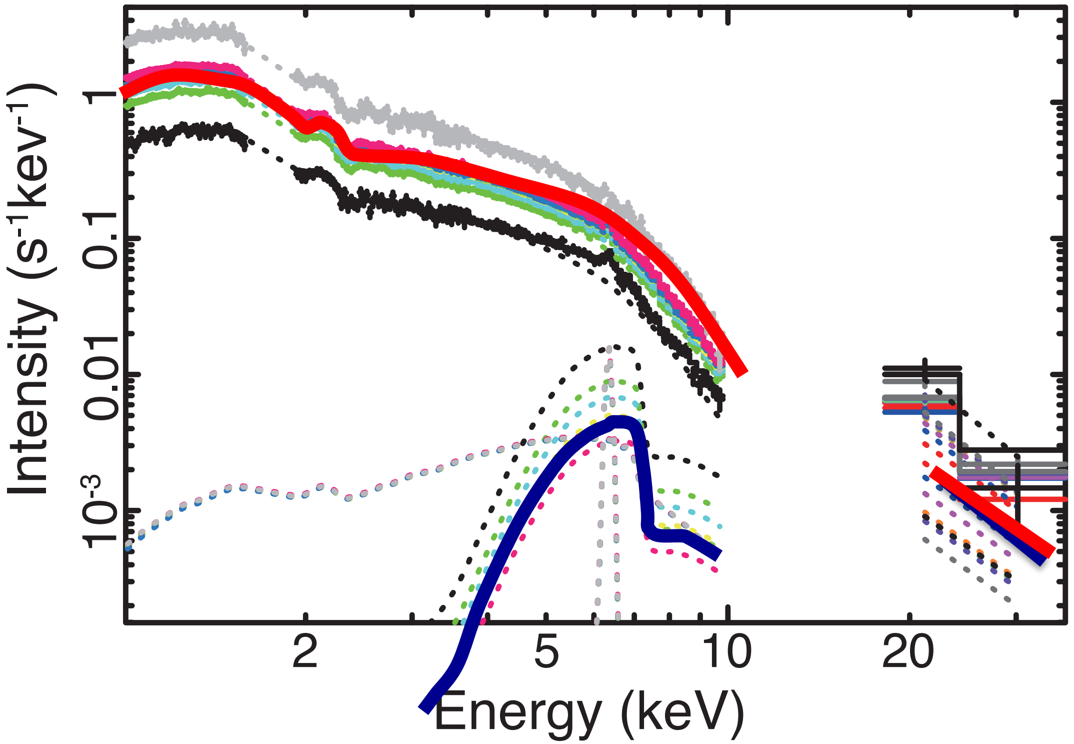


MCG-6-30-15 (Miyakawa, Ebisawa and Inoue 2012)

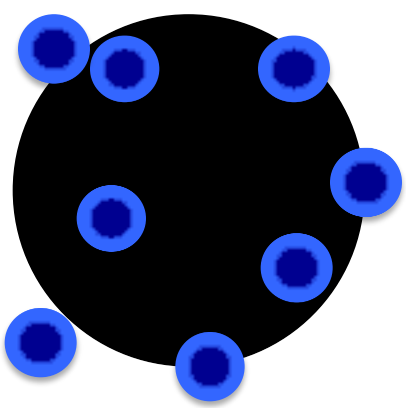

Covering fraction varies

# Variable Double Partial Covering Model

AGN luminosity and spectra below ~10 keV do not vary significantly within ~a day. Variation of the *partial covering fraction* explain most of the observed spectral variations below ~10 keV.

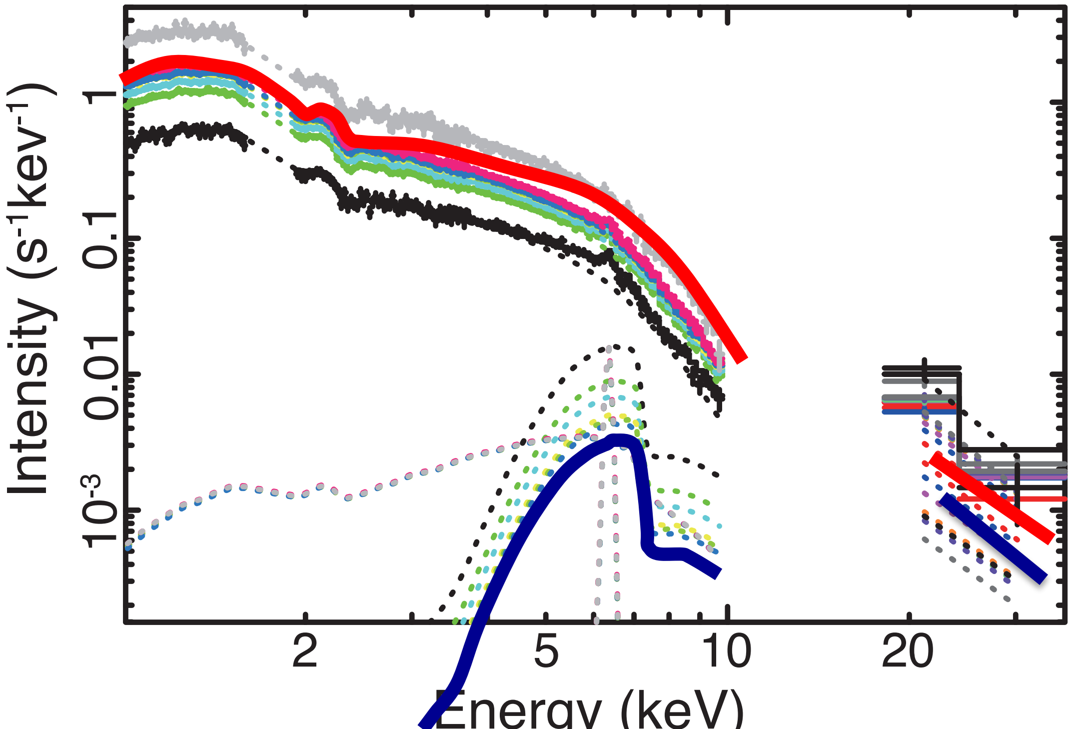


MCG-6-30-15 (Miyakawa, Ebisawa and Inoue 2012)

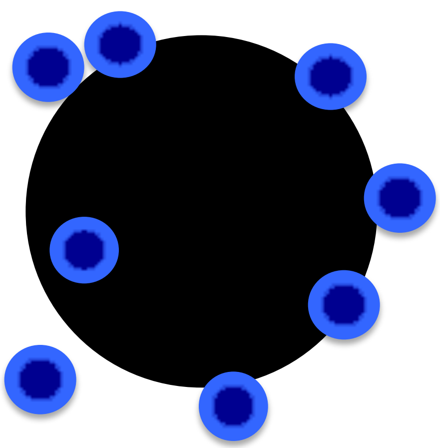

Covering fraction varies

# Variable Double Partial Covering Model

AGN luminosity and spectra below ~10 keV do not vary significantly within ~a day. Variation of the *partial covering fraction* explain most of the observed spectral variations below ~10 keV.

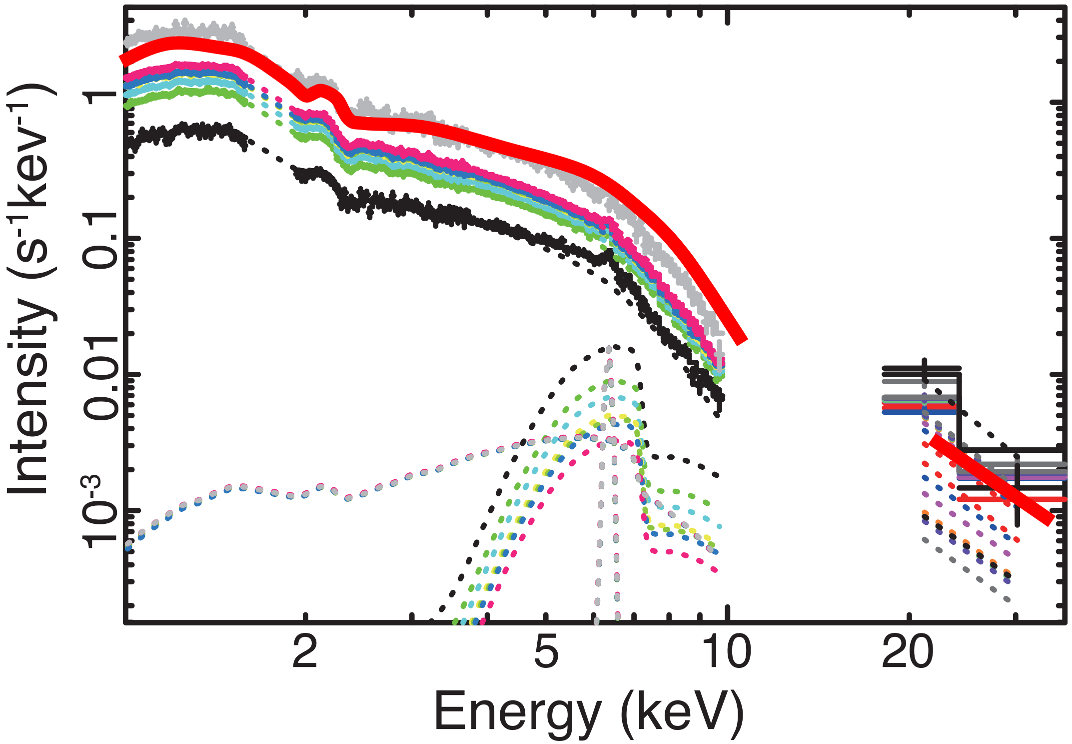


MCG-6-30-15 (Miyakawa, Ebisawa and Inoue 2012)

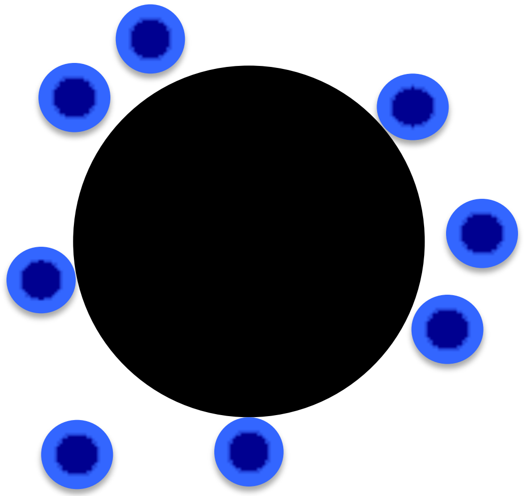

Covering fraction: Null

# Contents

# Contents

# 3. Application to Observations: spectral fits

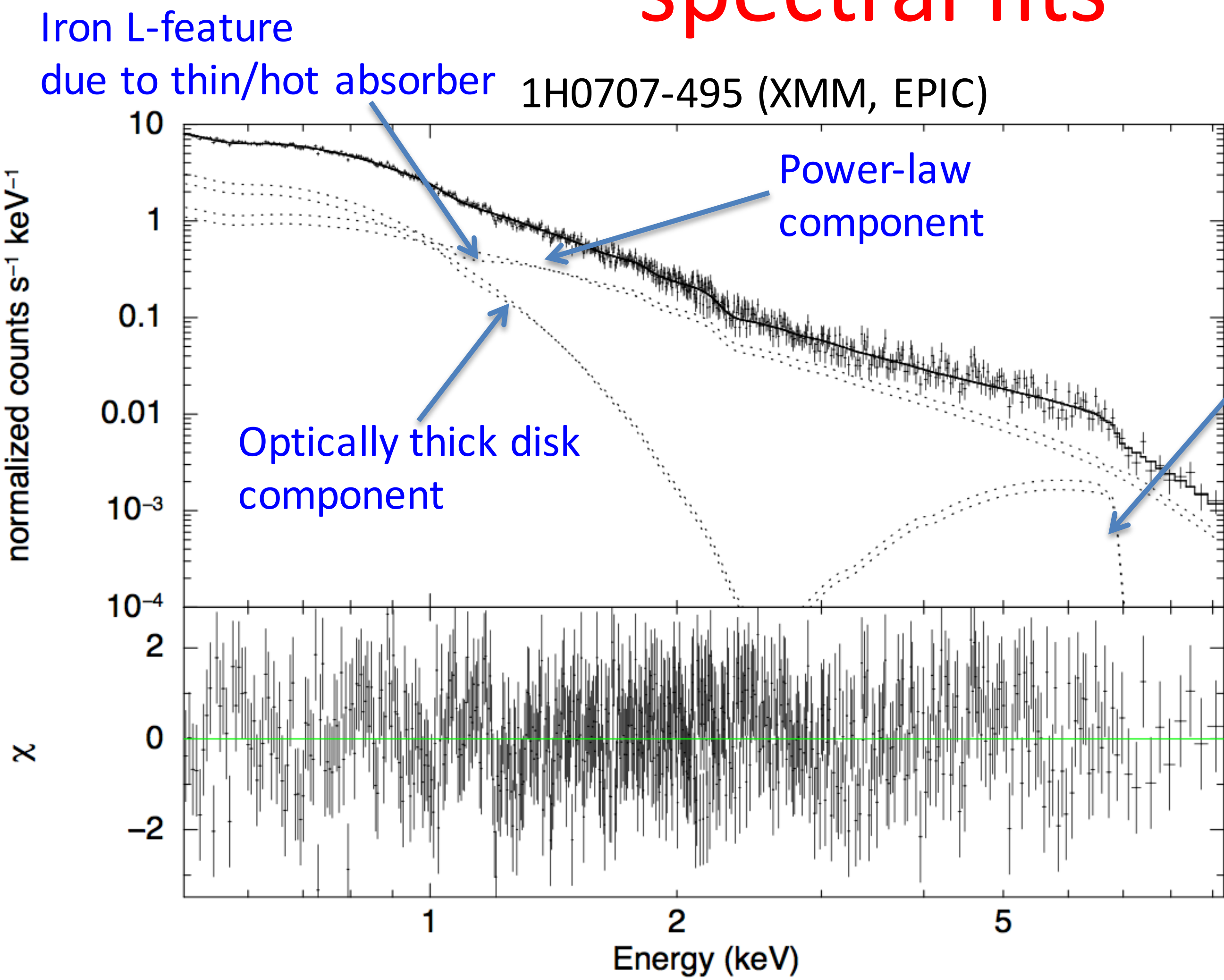


Thick/cold absorber:
$N_H \sim 10^{24} cm^{-2}$, $\xi \sim 10^{0.1-0.3}$

Thin/hot absorber:
$N_H \sim 10^{23} cm^{-2}$, $\xi \sim 10^{3}$

Mizumoto, Ebisawa and Sameshima (2014)

# 3. Application to Observations: flux-sorted spectral fits

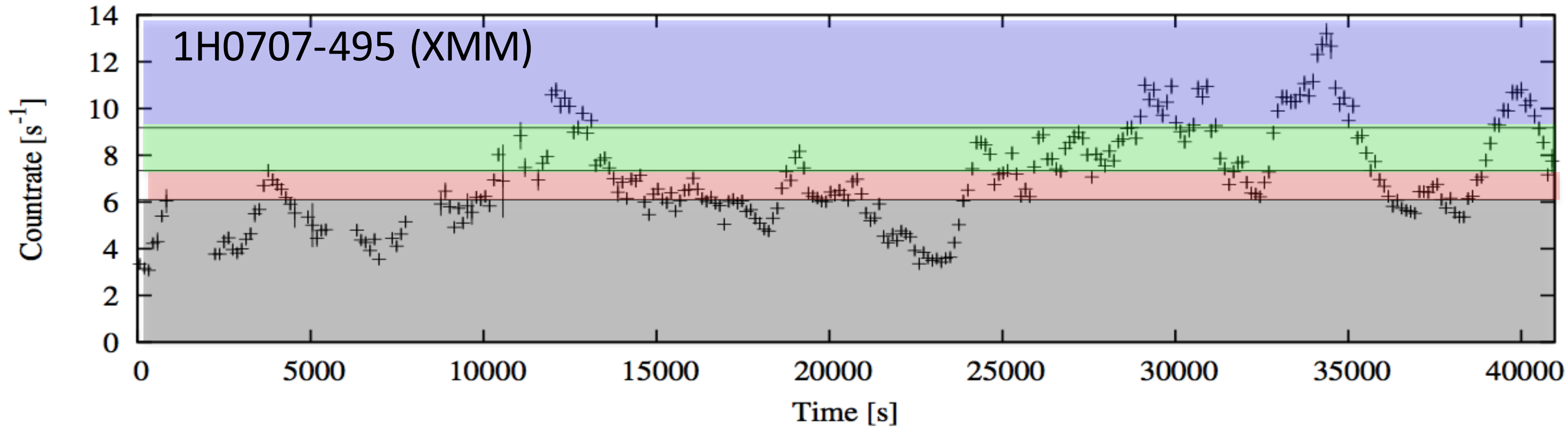


- Observation within ~a day is divided into four different flux levels
- Flux-sorted spectra below ~10 keV are fitted simultaneously only varying the partial covering fraction.

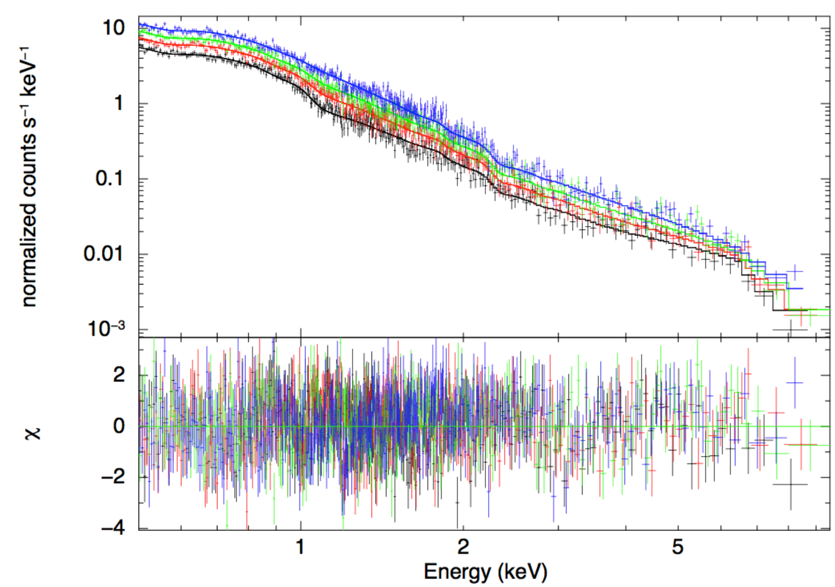


Mizumoto, Ebisawa and Sameshima (2014)

Flux-sorted spectra fitted simultaneously only varying the partial covering fraction.

Iso et al. (2016)

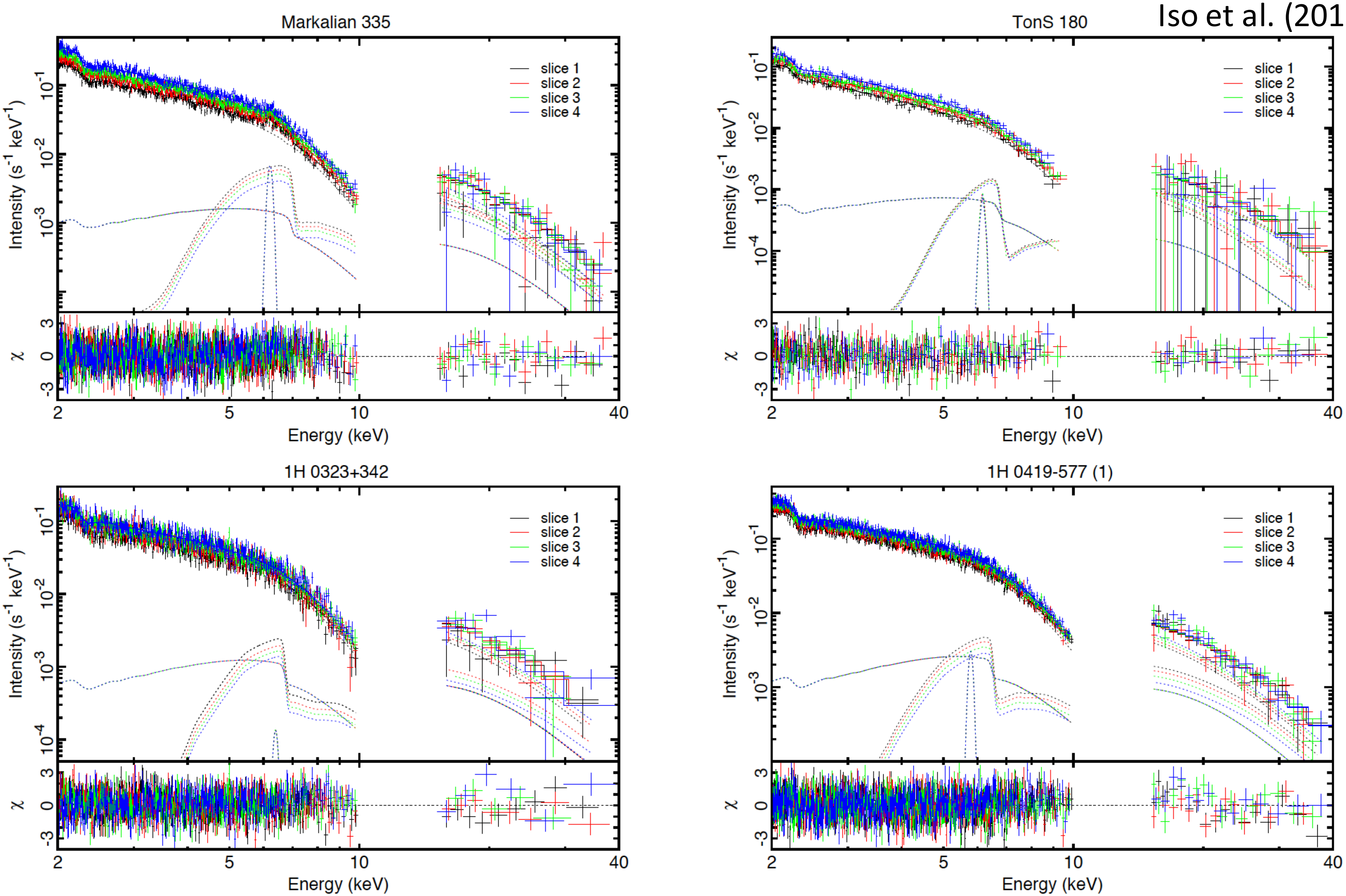

# Flux-sorted spectra fitted simultaneously only varying the partial covering fraction.

Iso et al. (2016)

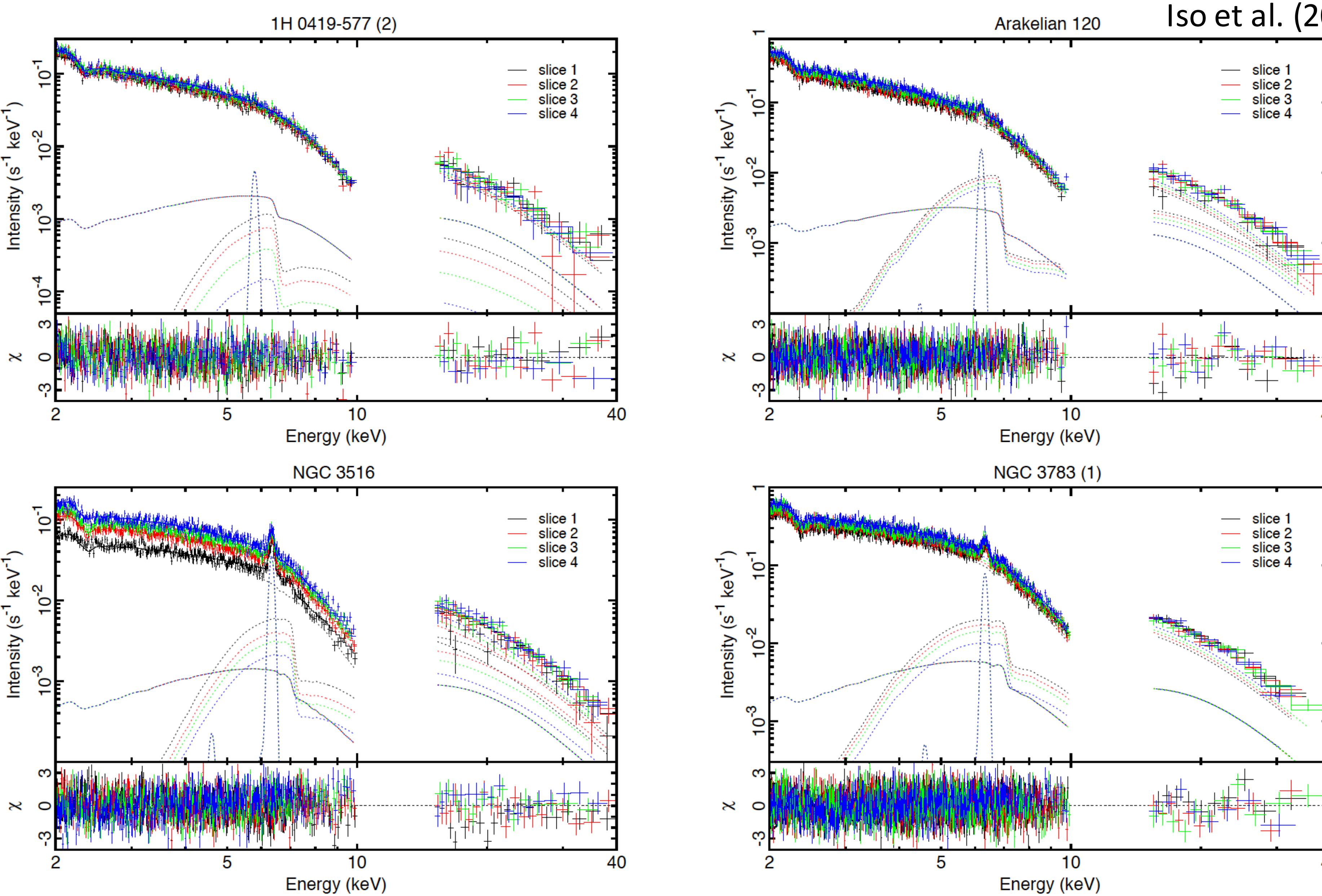

# Flux-sorted spectra fitted simultaneously only varying the partial covering fraction.

Iso et al. (2016)

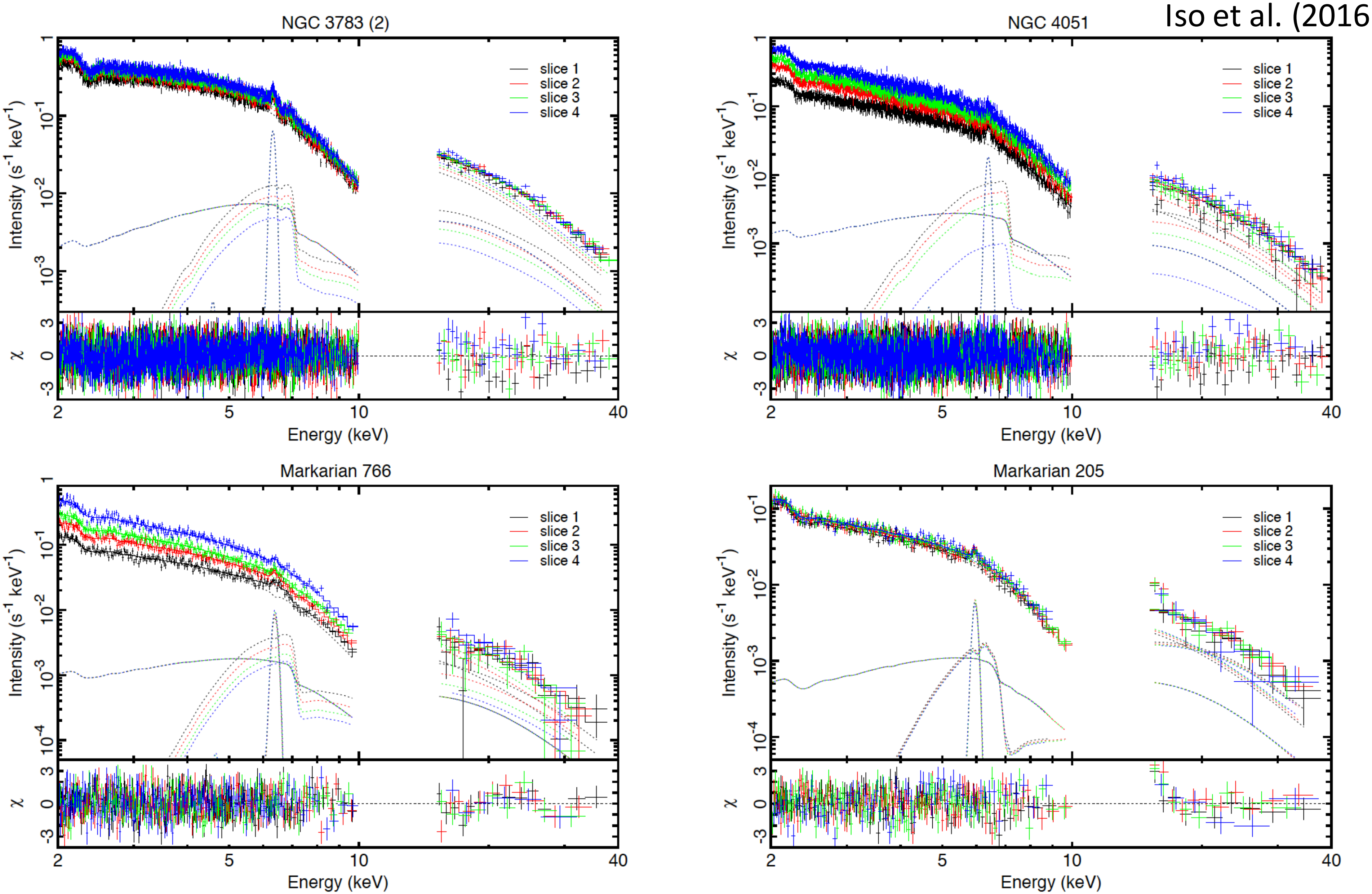

# Flux-sorted spectra fitted simultaneously only varying the partial covering fraction.

Iso et al. (2016)

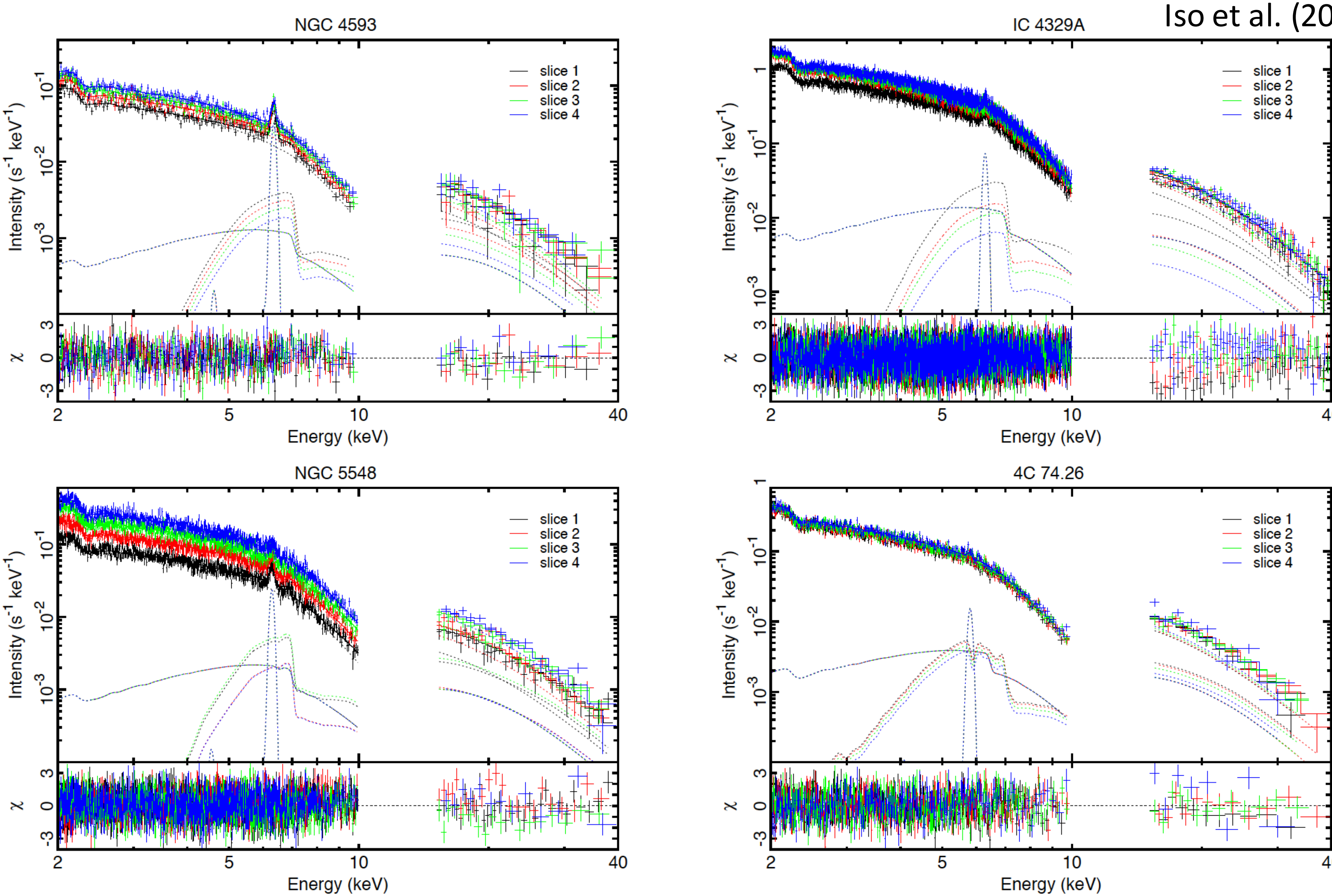

# Flux-sorted spectra fitted simultaneously only varying the partial covering fraction.

Iso et al. (2016)

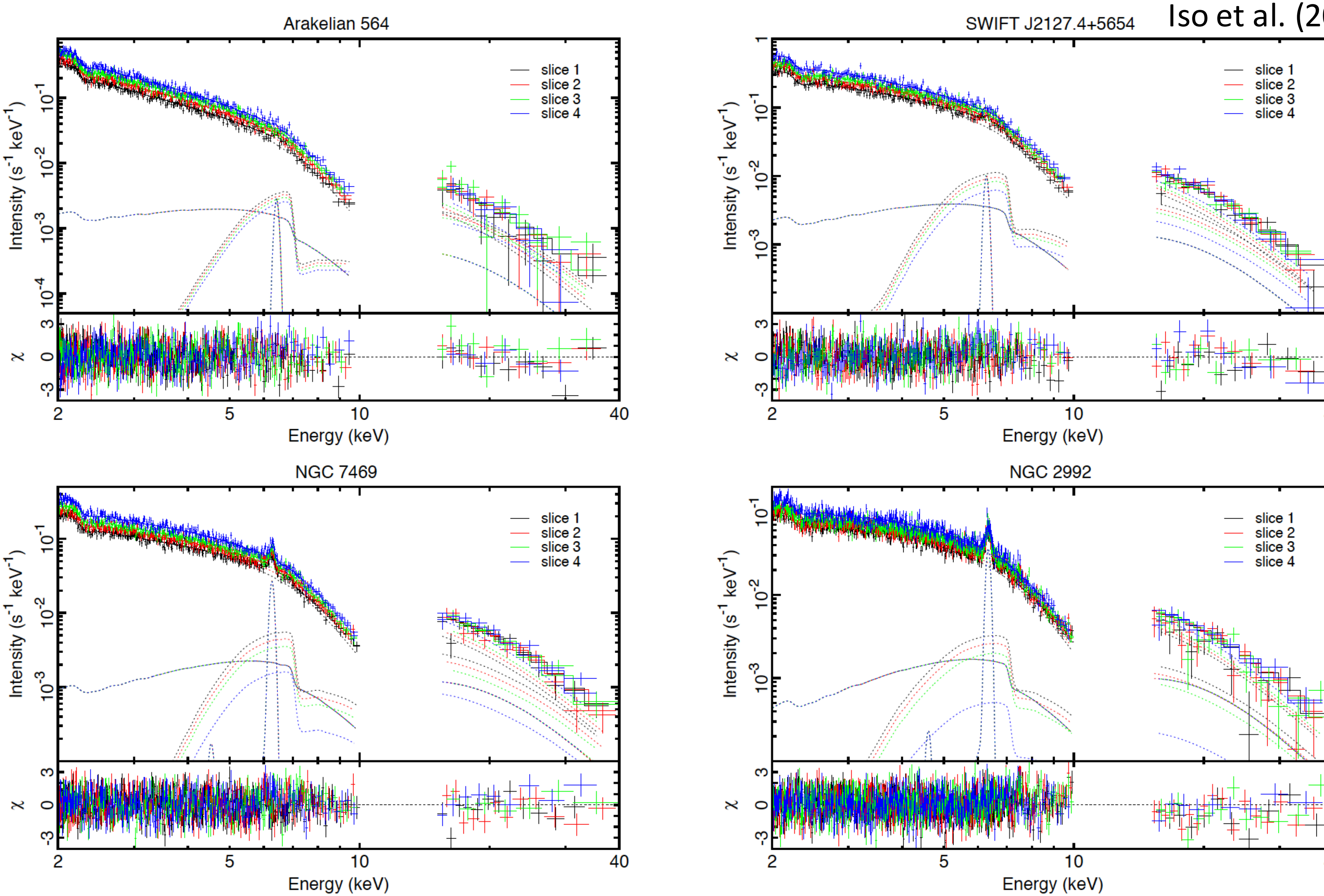

# Flux-sorted spectra fitted simultaneously only varying the partial covering fraction.

Iso et al. (2016)

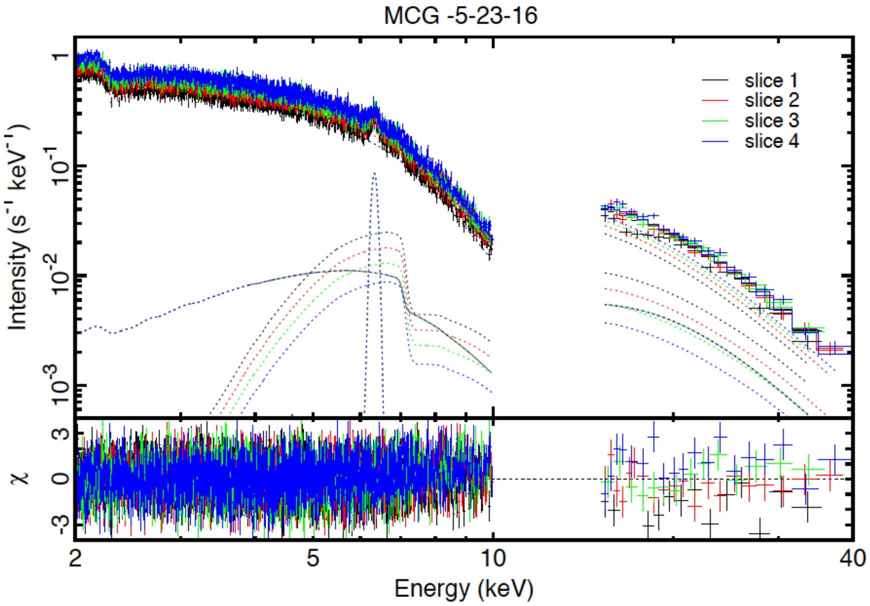


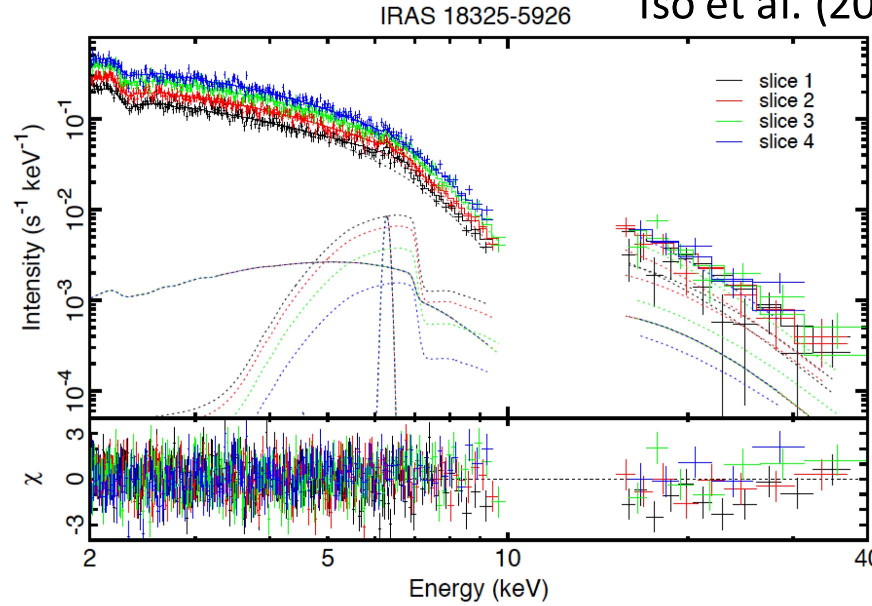

# 3. Application to Observations: Time-sliced spectra fits in 0.2-78 keV

- MCG6-30-15, XMM-NuSTAR simulteneous observation (2013/01/29 — 2013/02/02)

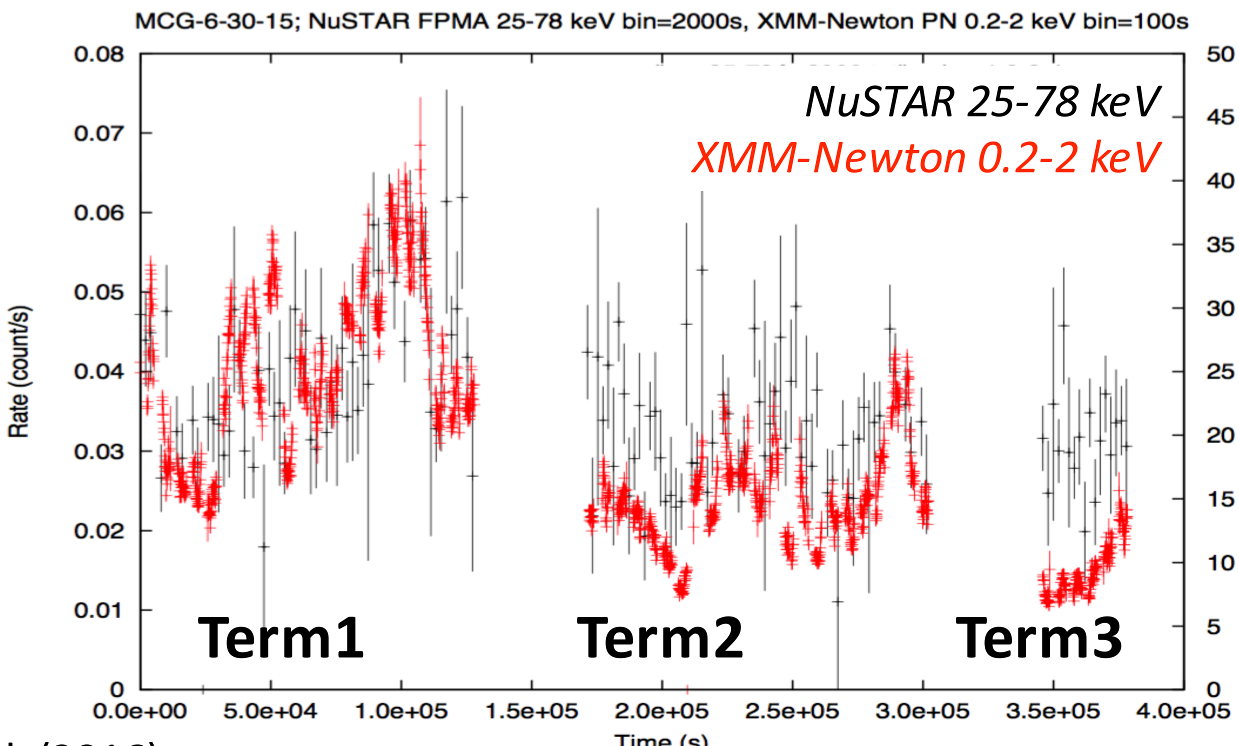


Kusunoki et al. (2016)

# Time-sliced spectra made every ~10ksec

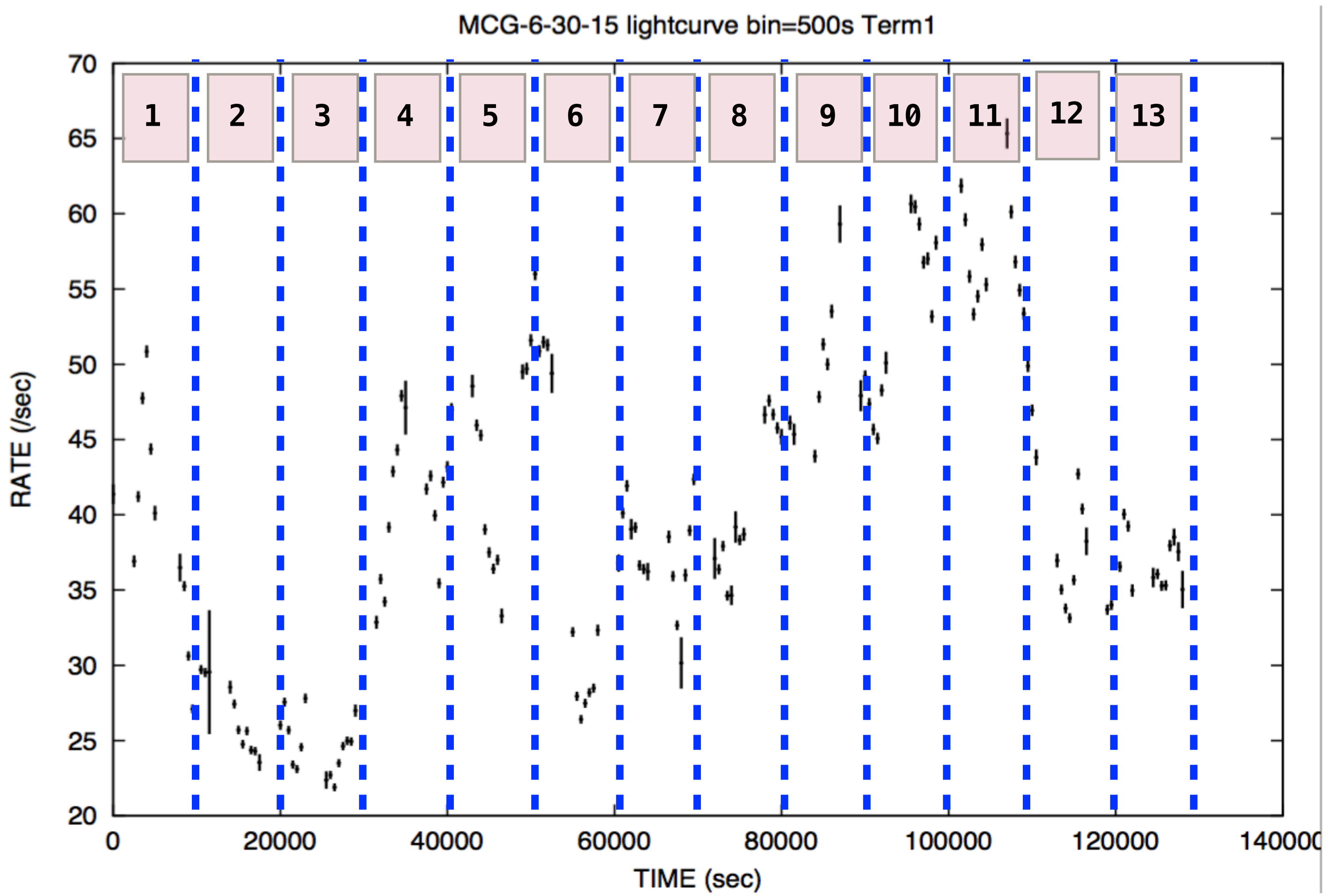


***XMM-Newton* 0.2-10 keV for Term1**

Kusunoki et al. (2016)

# Time-sliced spectra fitted simultaneously

$F = (\mathbf{PL}+diskbb) \times \{(1-\alpha + \alpha \exp[-\sigma(\xi_{low})N_{H,high}])(1-\alpha + \alpha \exp[-\sigma(\xi_{high})N_{H,low}])$

$+ Reflection \} \times \exp[-\sigma(\xi_{high})N_{H,low}]$

Power law normalation [PLnorm] is determined from 25-78 keV)

The partial covering fraction [$\alpha$] is a free-parameter

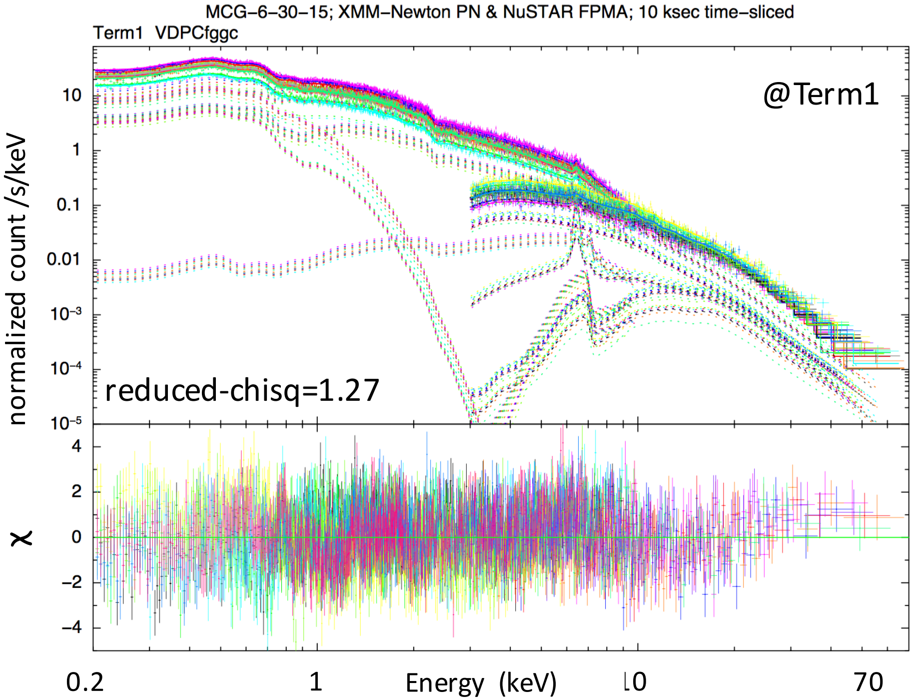


For each Term, the time-sliced spectra are fitted simultaneouly

Spectral variation in 0.2-78 keV is explained by only two variable parameters

Kusunoki et al. (2016)

# Variation of the two parameters

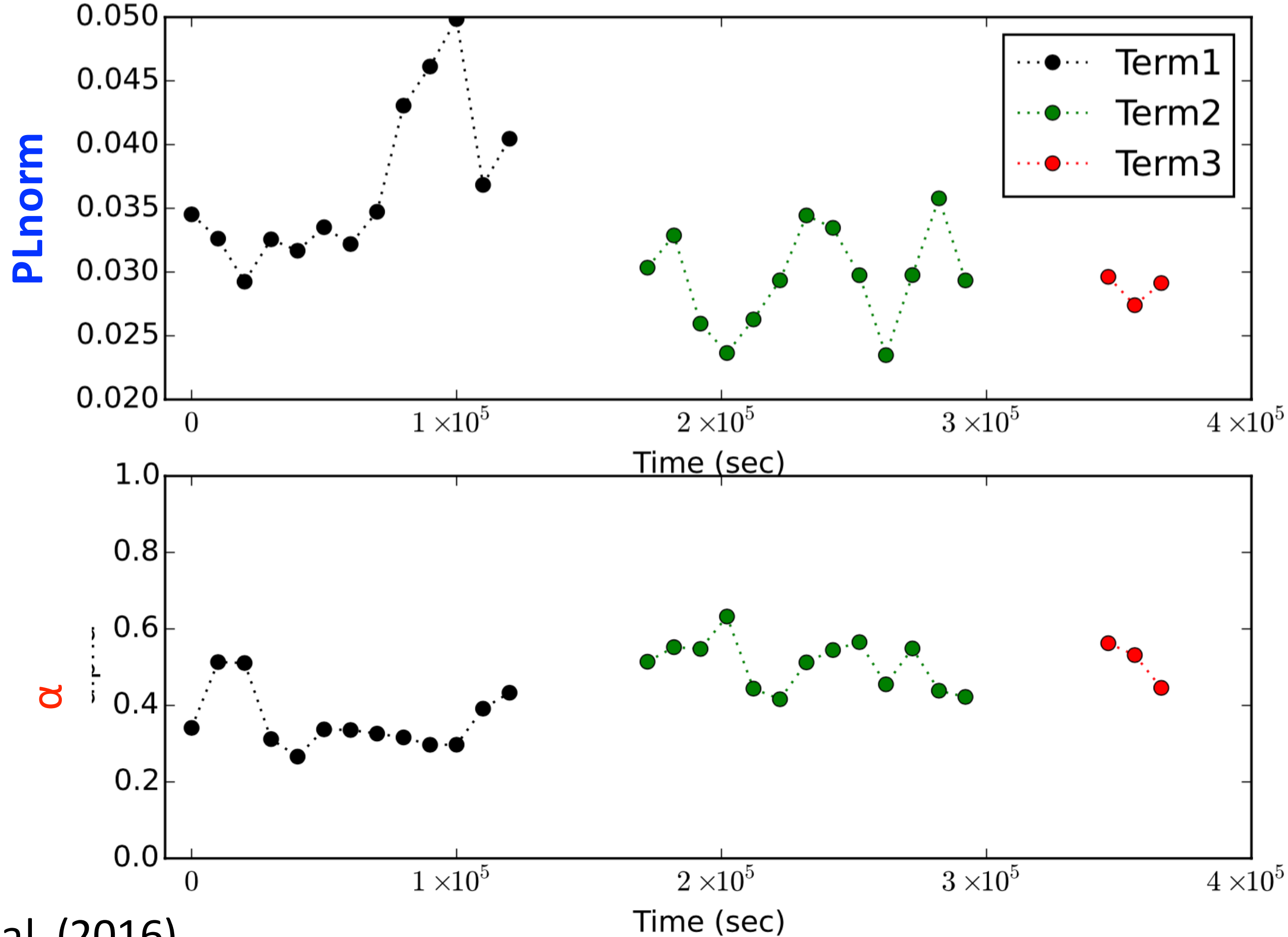


Kusunoki et al. (2016)

*Partial covering fraction and power-law normalization are independently variable*

# 3. Application to Observations: RMS spectra in iron K-band

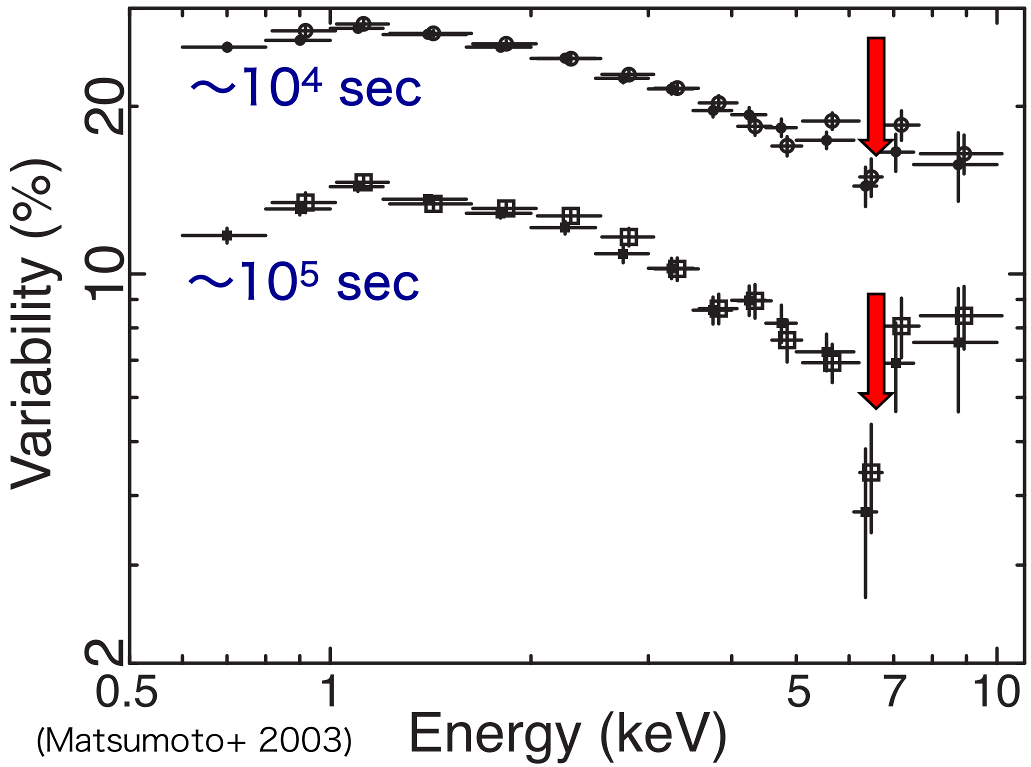


(Matsumoto+ 2003)

- MCG-6-30-15 with ASCA
  Energy dependence of Root Mean Square (RMS) variation
- RMS spectra of the Seyfert galaxies with broad iron features show significant drop at the iron K energy band

# 3. Application to Observations: RMS spectra in iron K-band

- In the VDPC model, variations of the direct component and the absorbed component cancel each other
- This is effective in the iron K- energy band

# 3. Application to Observations: RMS spectra in iron K-band

- In the VDPC model, variations of the direct component and the absorbed component cancel each other
- This is effective in the iron K- energy band

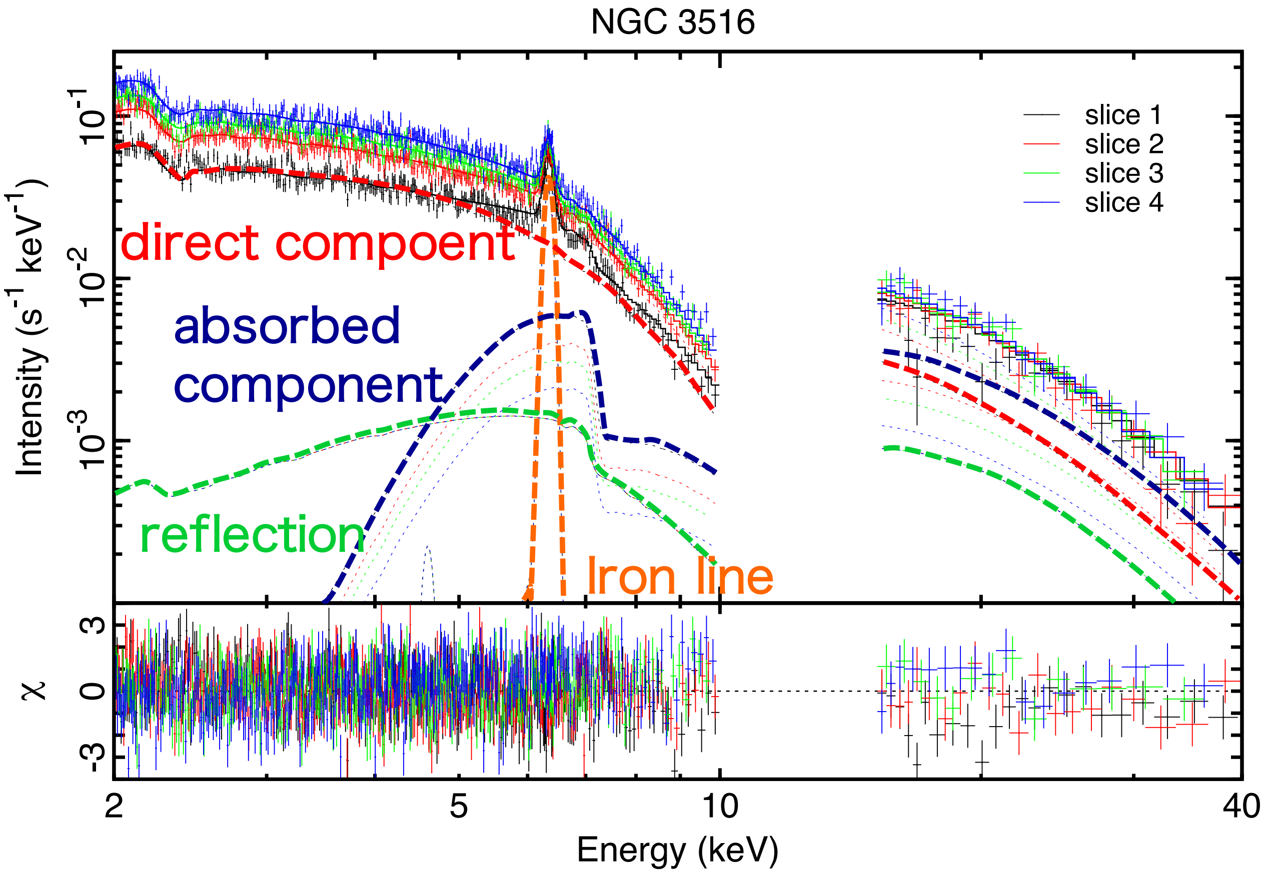


Iso et al. (2016)

# 3. Application to Observations: RMS spectra in iron K-band

- Observed Root Mean Square spectrum is explained by only variation of the covering fraction

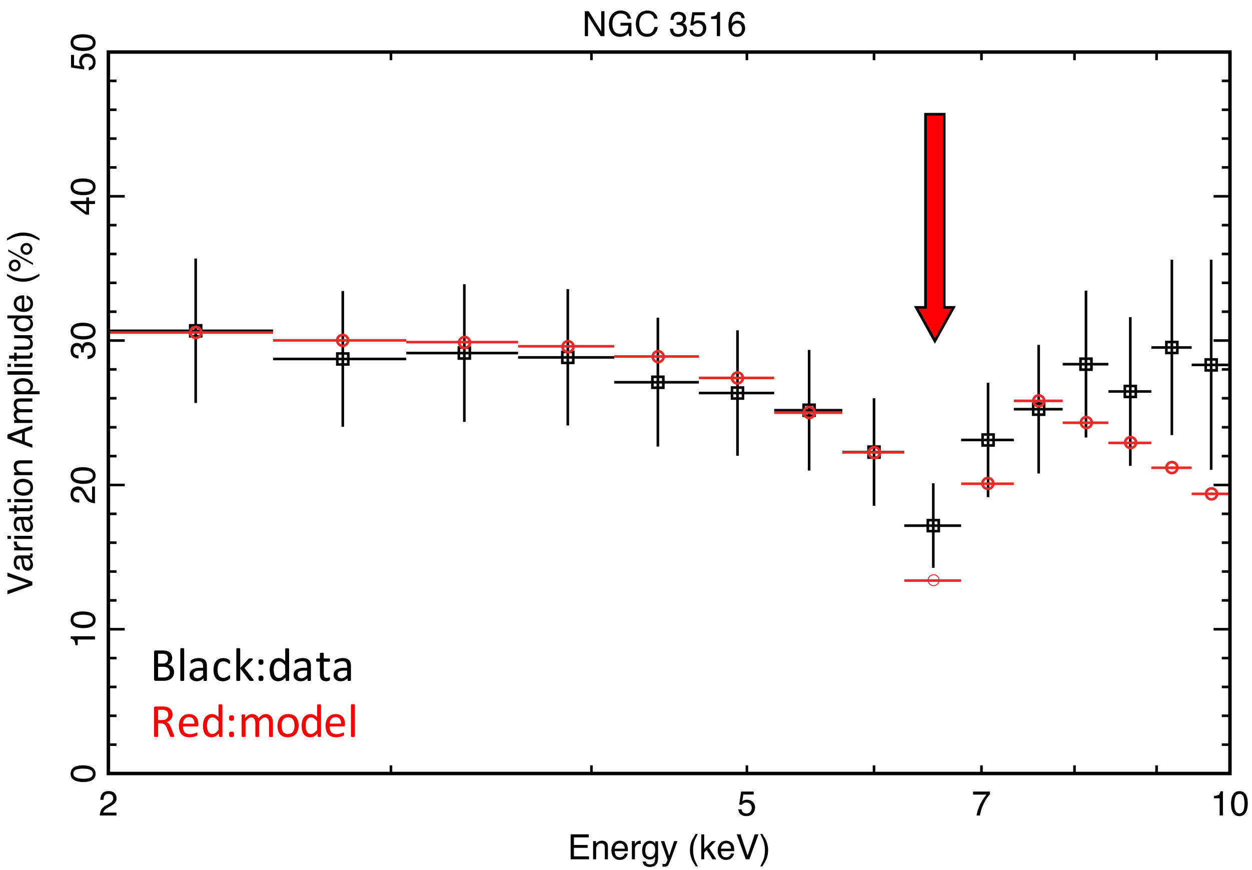


Iso et al. (2016)

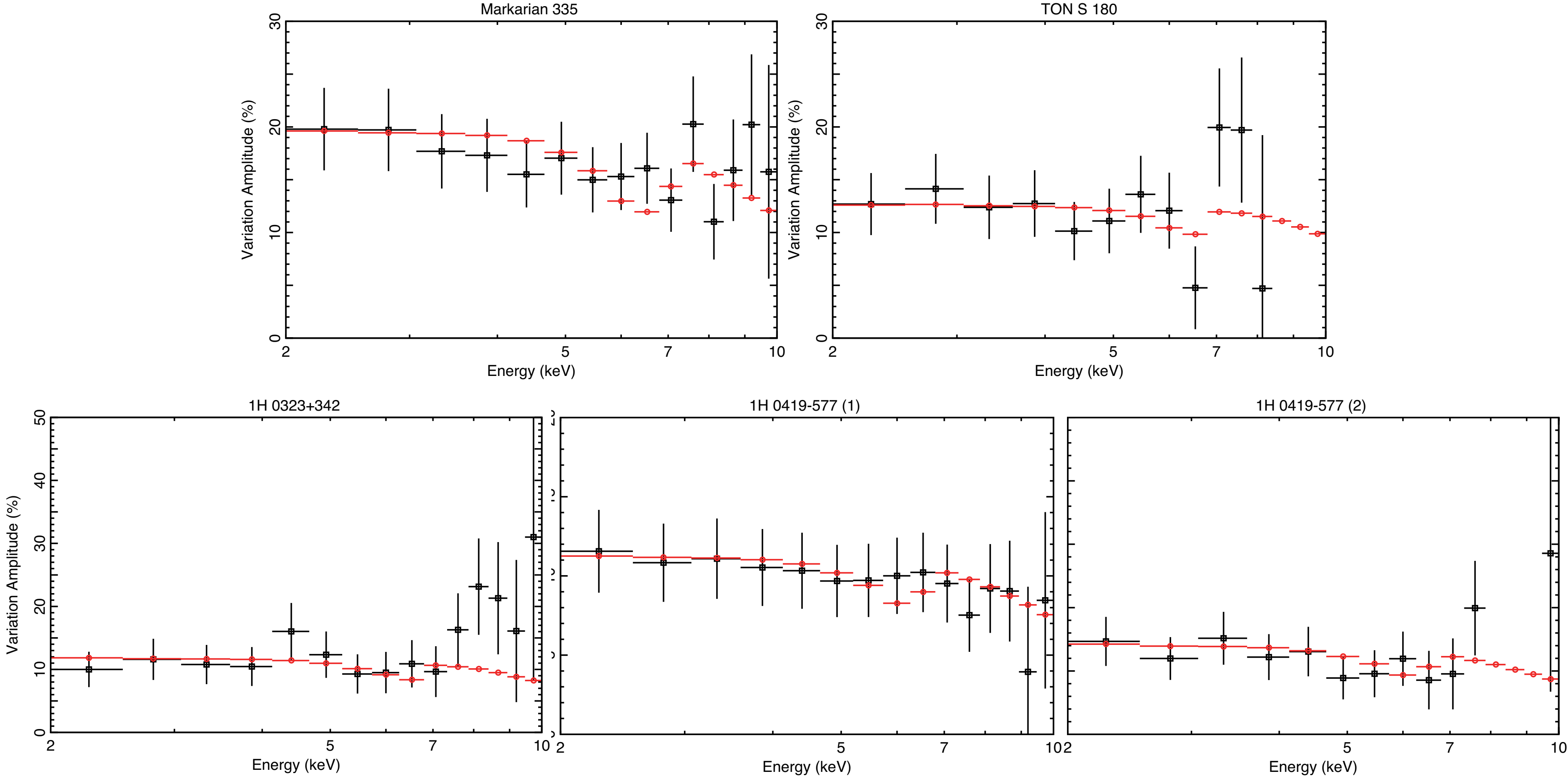


Example of
other sources
Black:data
Red:model

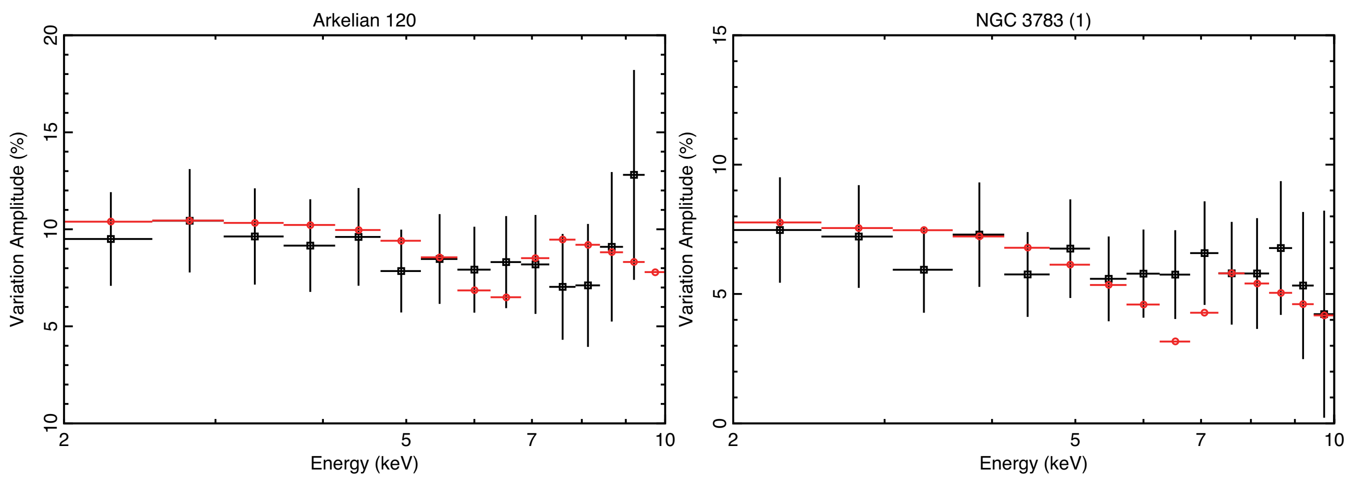


Iso et al.
(2016)

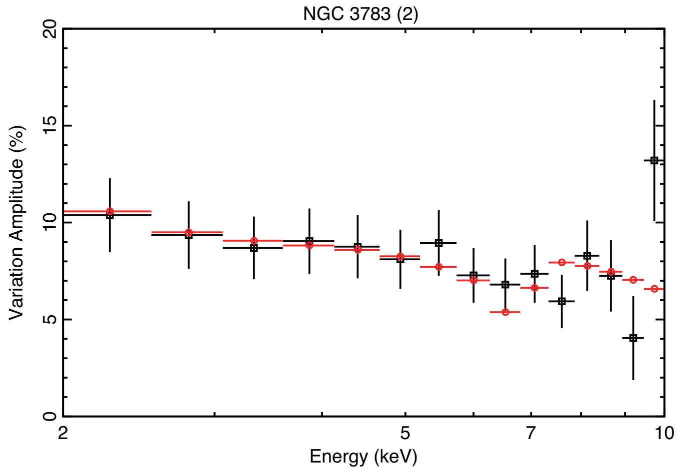

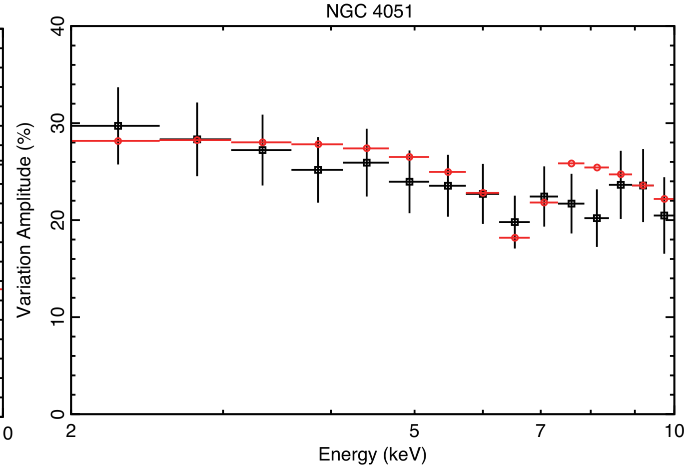

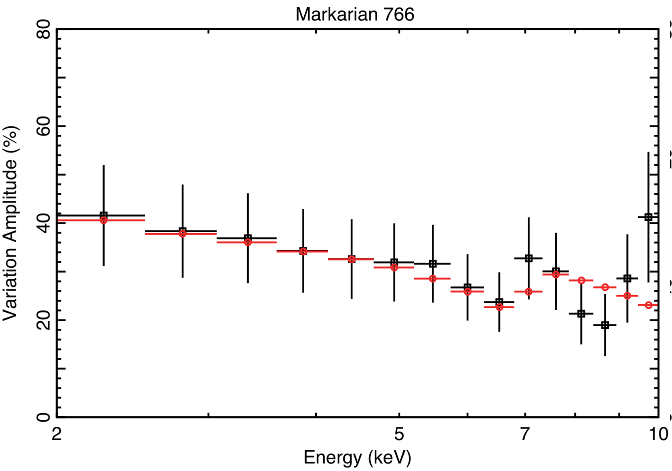

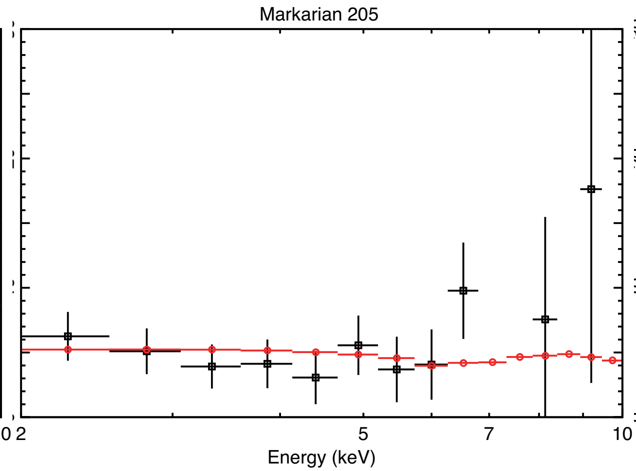

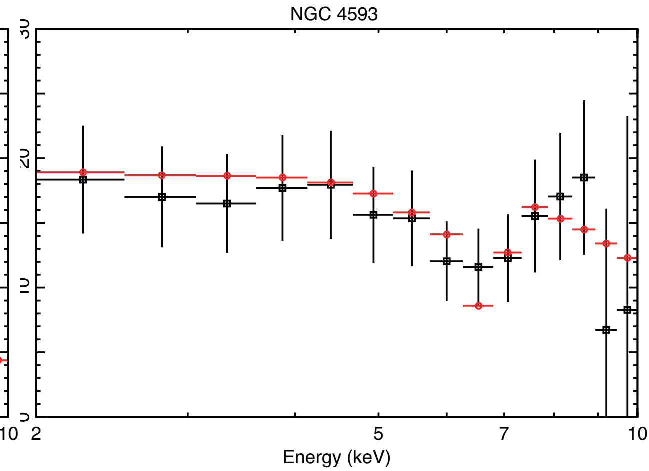


Example of other sources
Black:data
Red:model

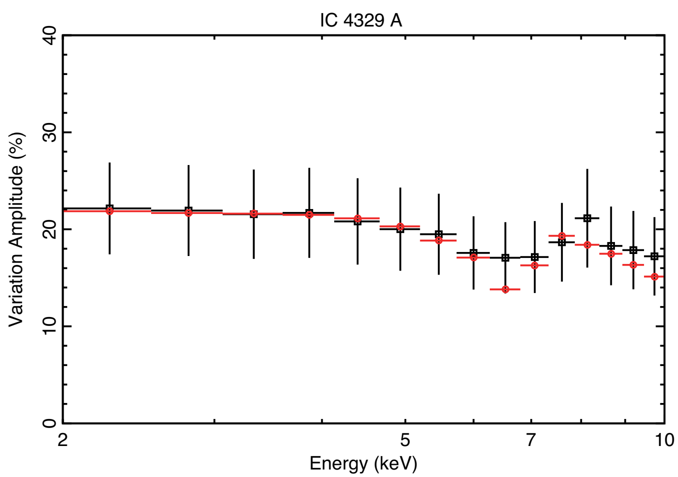

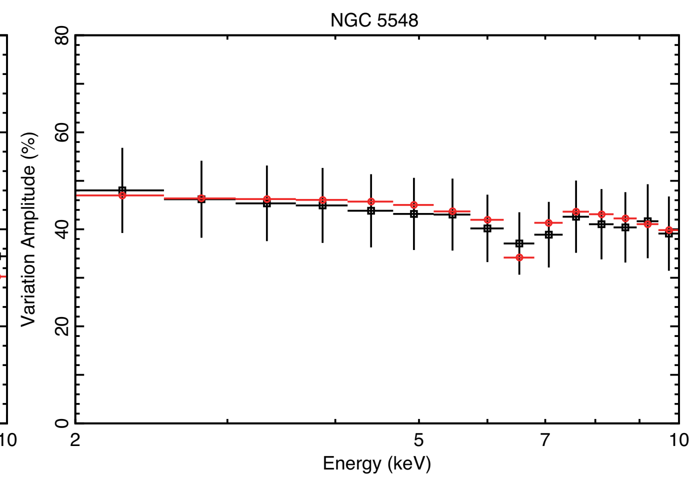


Iso et al. (2016)

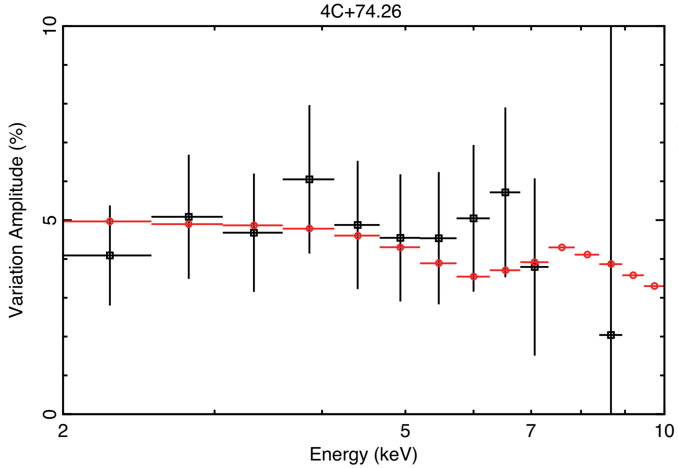


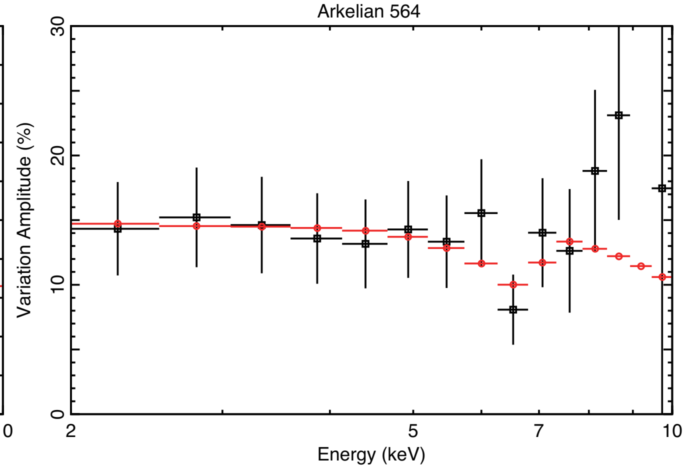


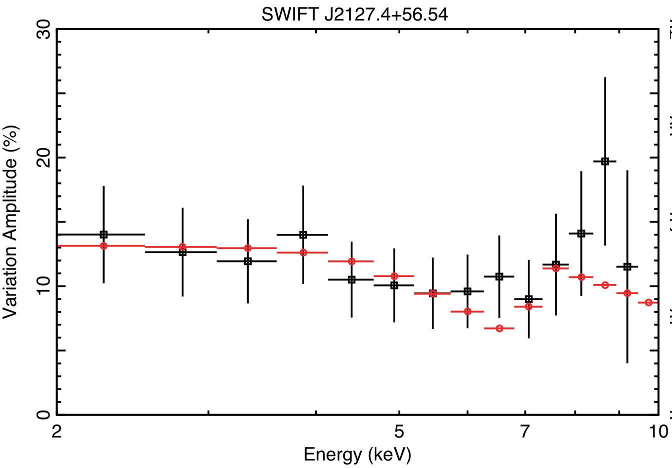


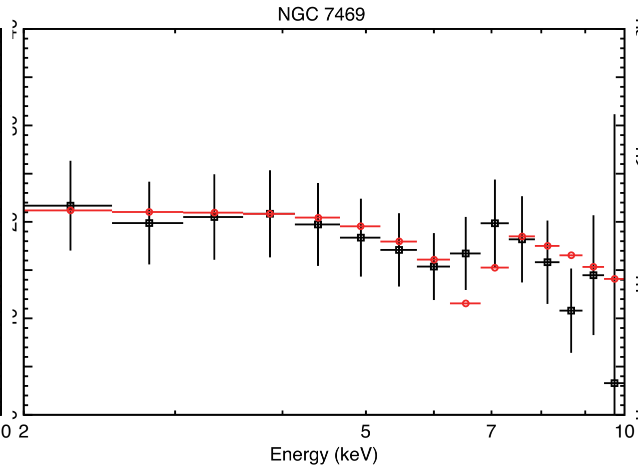


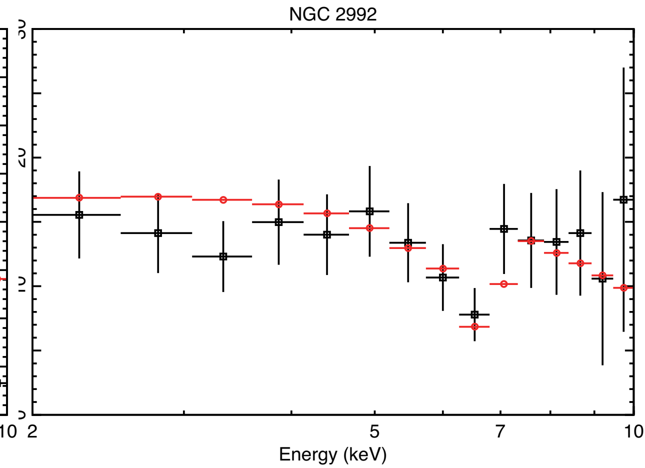


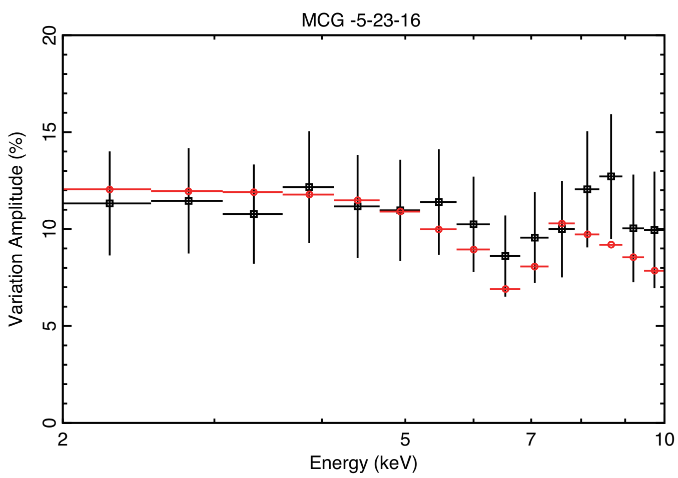


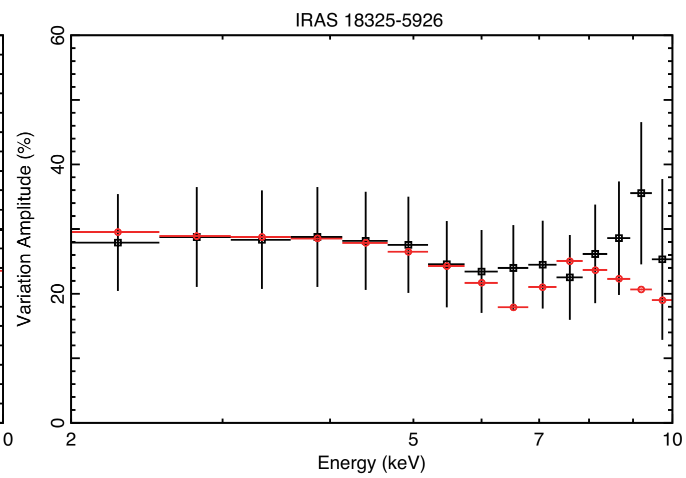


Example of other sources
Black:data
Red:model

Iso et al. (2016)

# Characteristic iron-L feature in the RMS spectra

- Iron L-peaks are seen in the RMS spectra when iron L-absorption edges are particularly strong.

Yamasaki et al. (2016)

# Characteristic iron-L feature in the RMS spectra

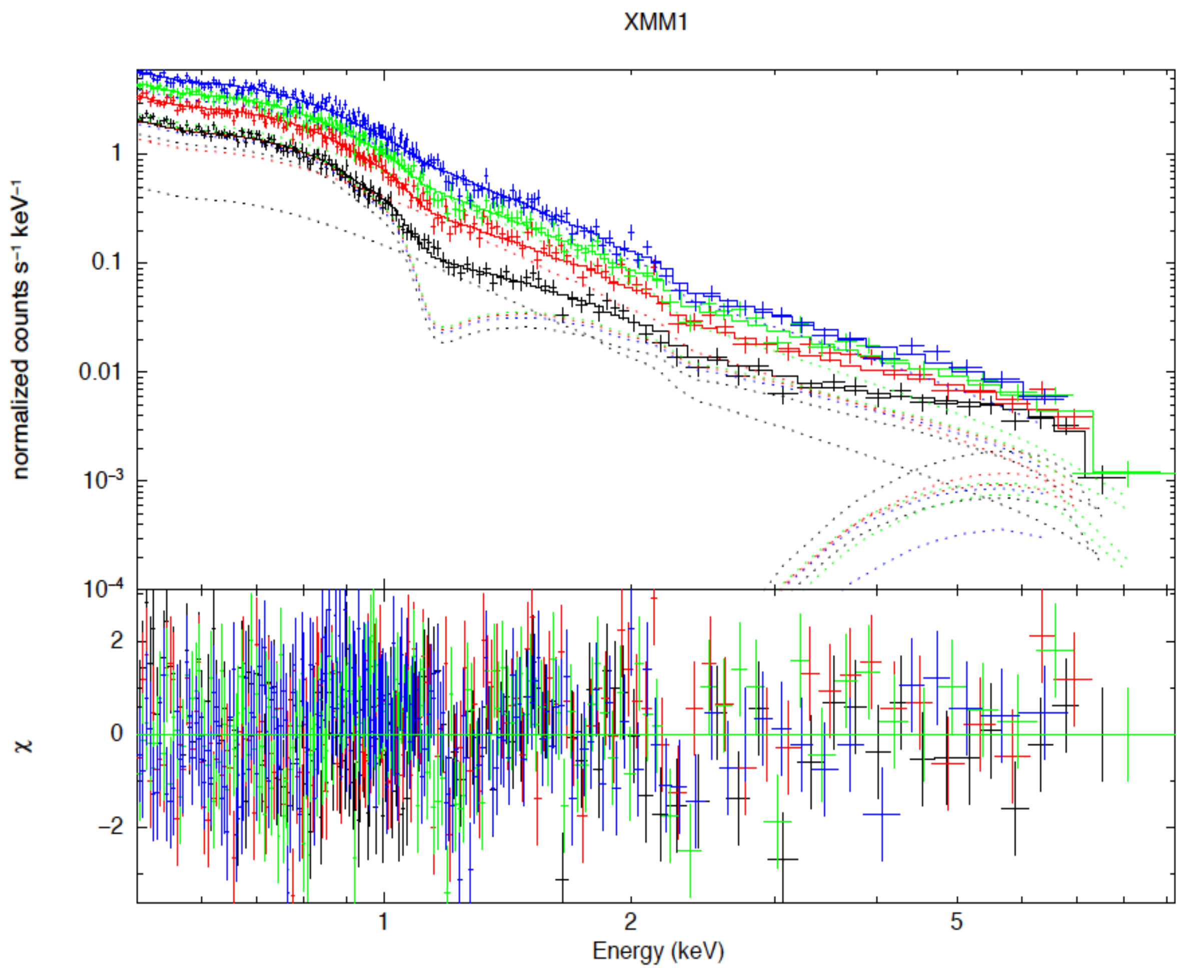


ꓤAS13224-3809

...ki et al. (2016)

# Characteristic iron-L feature in the RMS spectra

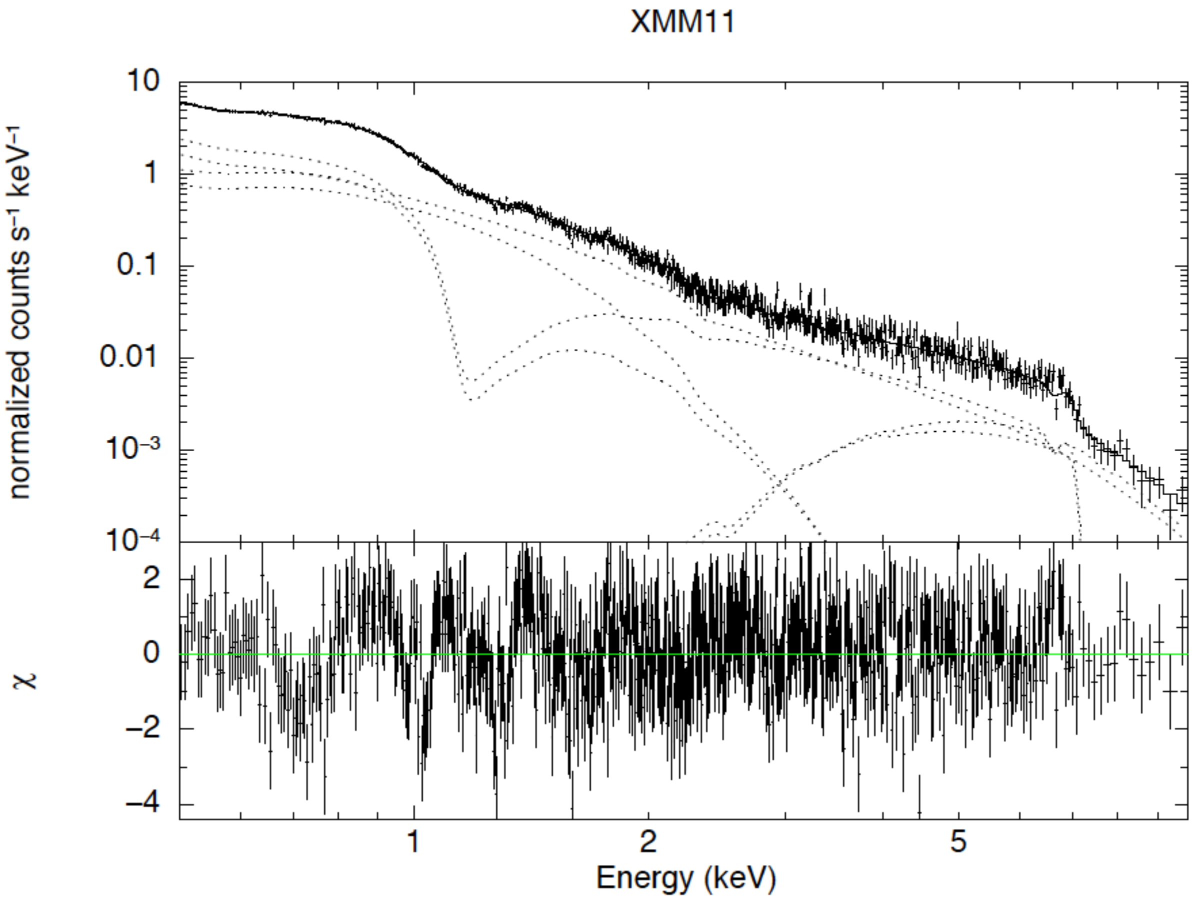


1H0707-495

Yamasaki et al. (2016)

# Explanation of the RMS spectra with the VDPC model

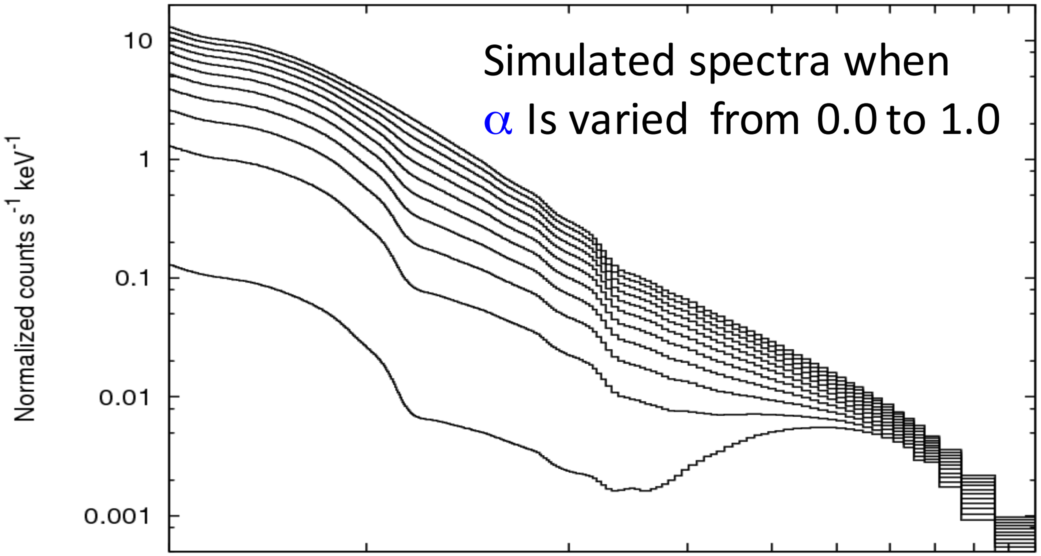


$$(1-\alpha+\alpha\exp(-N_H^{(k)}\sigma(\xi_k))$$
$$\times$$
$$(1-\alpha+\alpha\exp(-N_H^{(n)}\sigma(\xi_n))$$

where $\alpha$ is the partial covering fraction

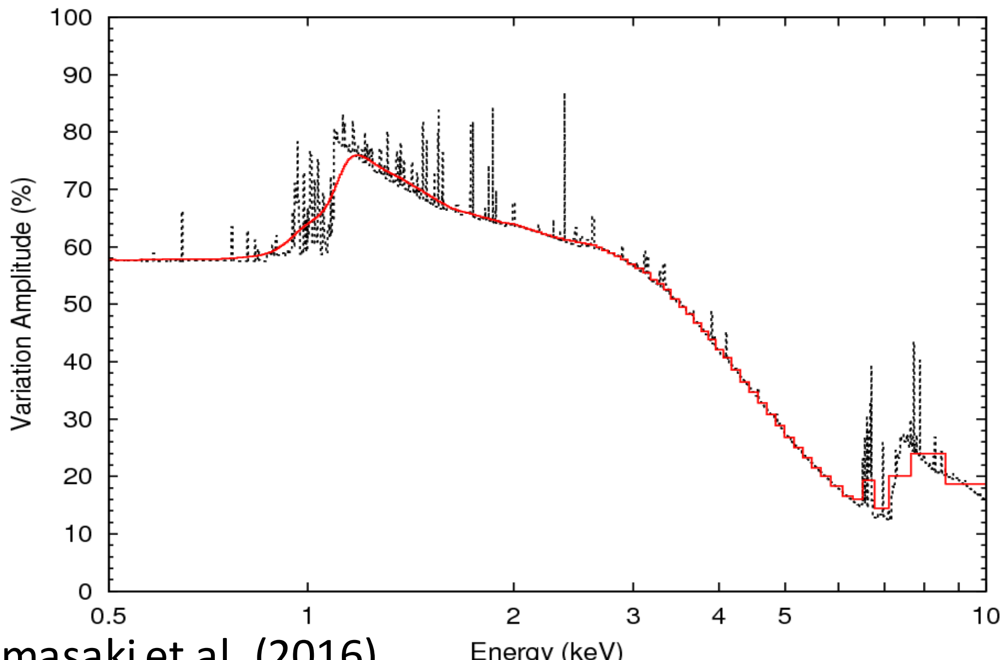


Yamasaki et al. (2016)

Model RMS spectrum

Peaks appear where the optical-depth is large (L-edge, K-edge, absorption lines)

The deepest valley is where the optical depth is the smallest (i.e. just below the iron K-edge)

Explain observed RMS spectra

# Explanation of RMS spectrum

- From RMS spectra with high spectral resolutions, we may separate different absorption layers

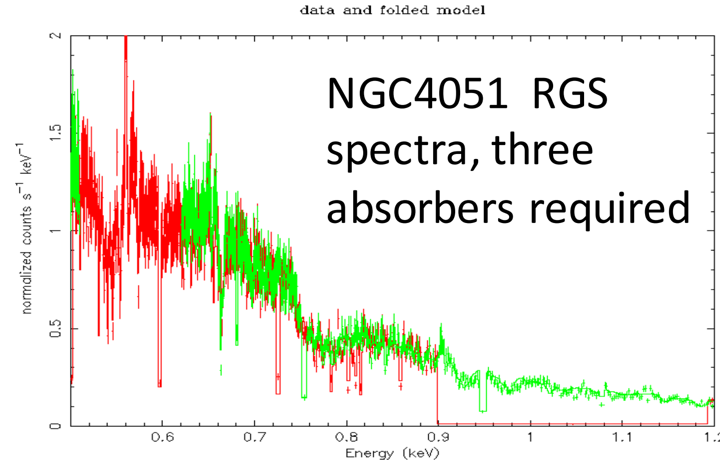


Mizumoto and Ebisawa (2016)

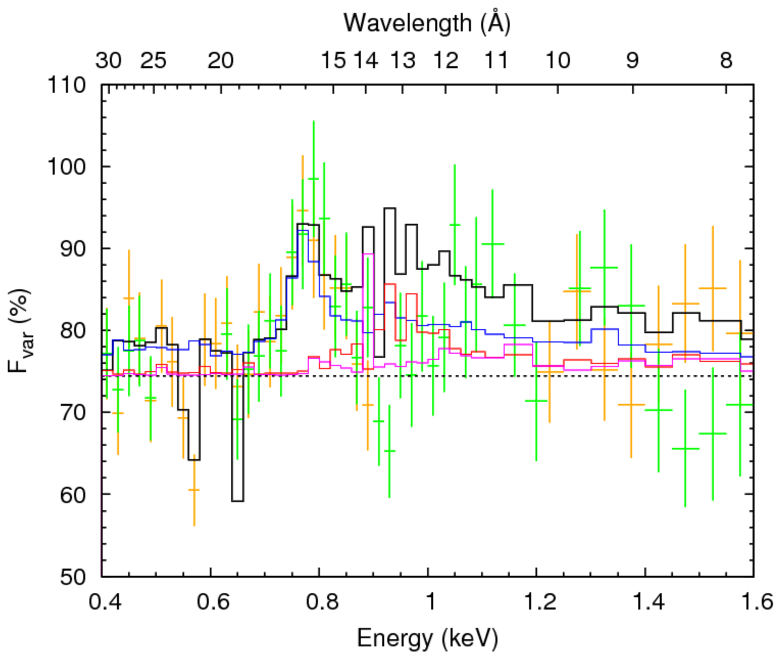


RMS spectrum does not fit with variable three absorption layers

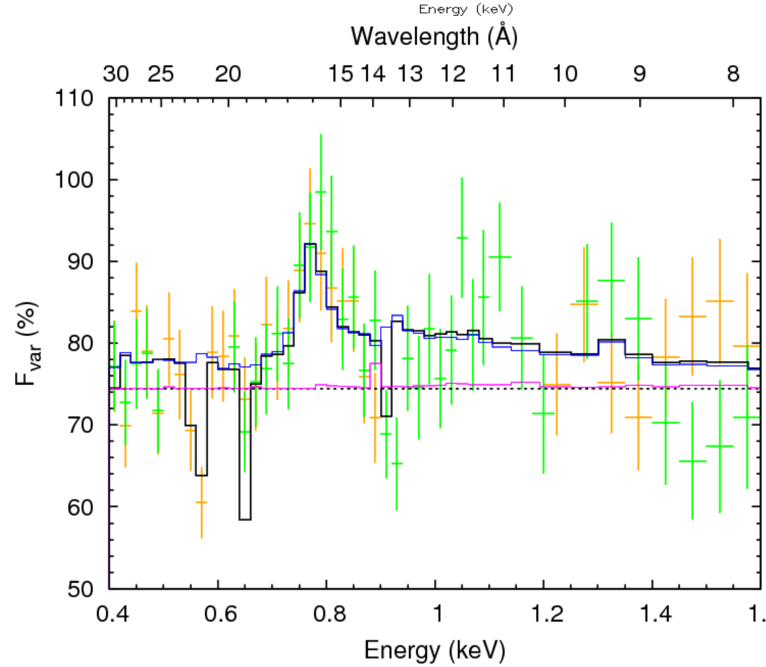


Fit with a single variable absorption layer and two static layers

# 3. Application to Observations: light curves

- We examine if light curves (512 sec bin) in different energy bands are explained by the VDBC model.
- From the 0.5-10 keV counting rates, we calculate $\alpha$ for each bin, from which we calculate model light curves in  0.5-1.0 keV (Soft), 1.0 keV-3.0 keV (Medium) and 3.0-10 keV (Hard).
- Compare the simulate light curves in the three energy bands with the observed ones.

1E0707-495 with XMM

Red: model

Black: data

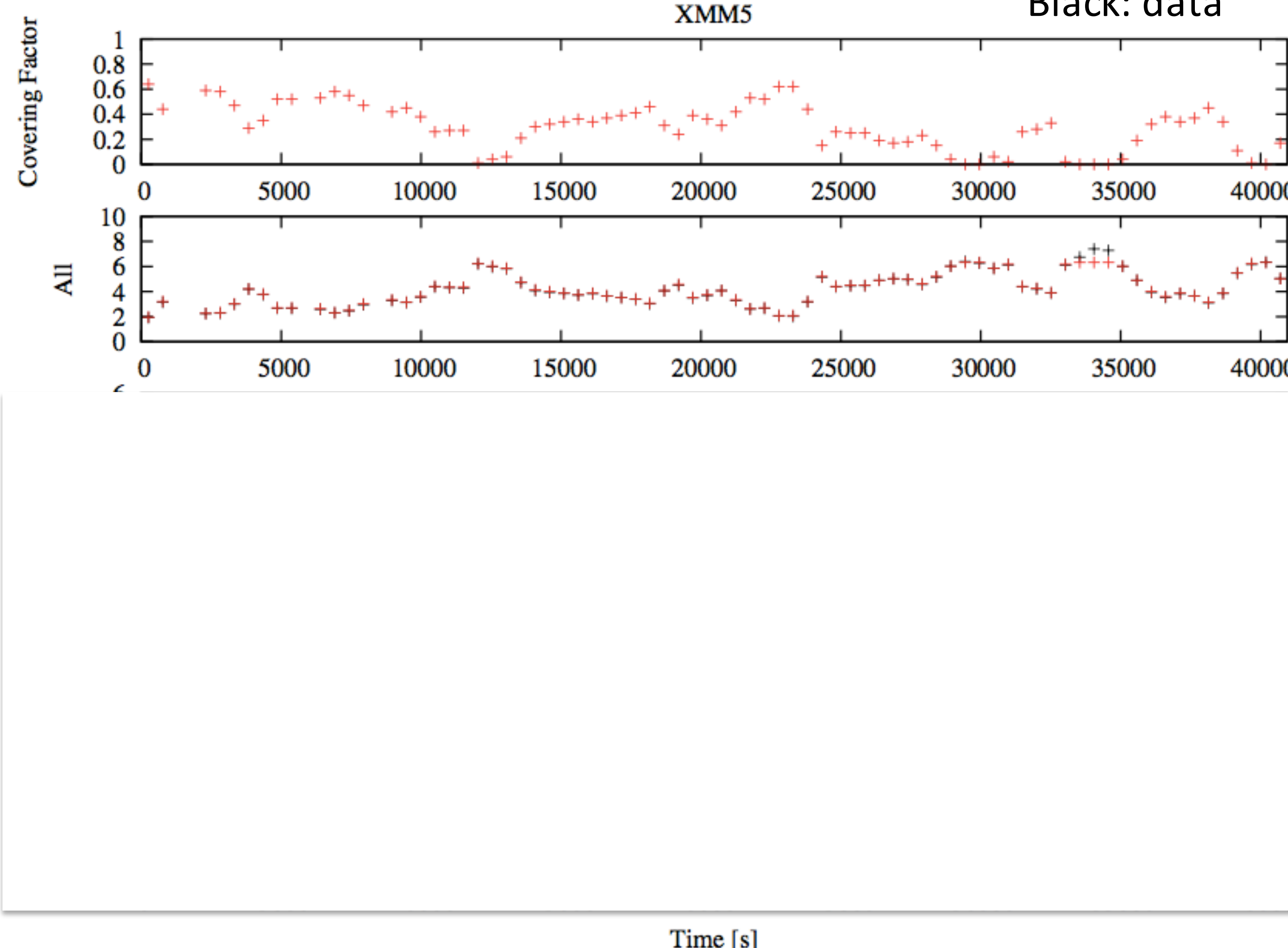


Mizumoto, Ebisawa and Sameshima (2014)

Red: model
Black: data

IRAS13224-3809 with XMM

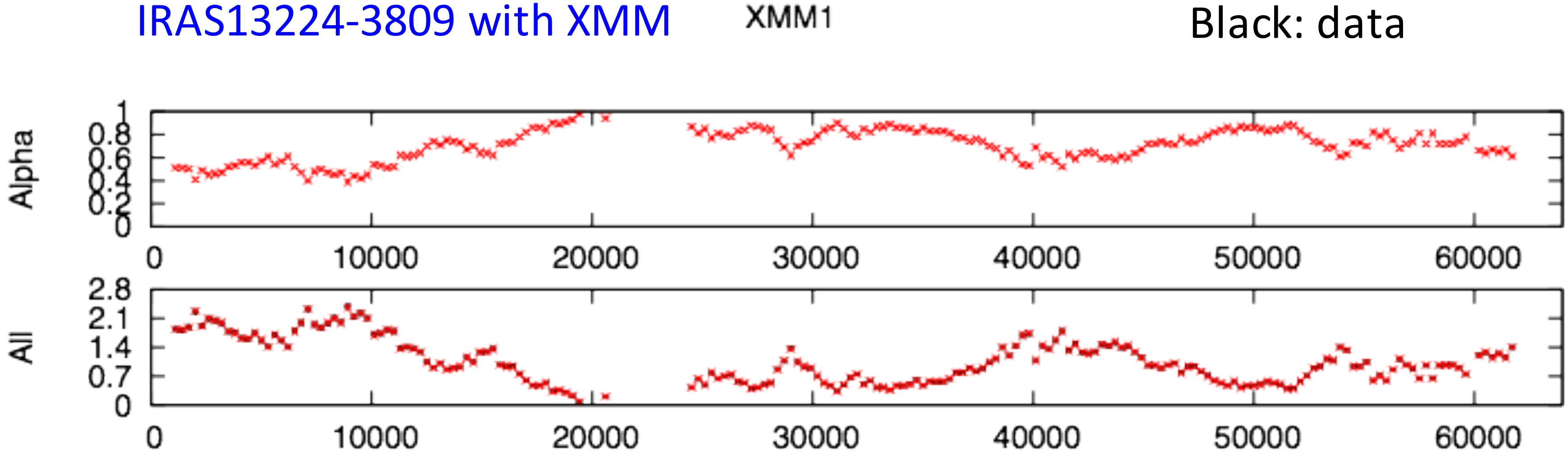


Yamasaki et al. (2016)

# 3. Application to Observations: light curves

- Soft band (0.5-1.0 keV) light curves are explained by the VDPC model.
- Agreement between model and data is reasonable in Medium (1.0-3.0 keV) and Hard (3.0 -10keV) band, but worse in higher energies.
- Deviation in the Hard band is due to intrinsic variation of the hard spectral component (Kusunoki et al. 2016).

# Contents

# Contents

# 4. Structure around the AGN

- Covering fraction can be large ($\alpha$>0.9) in the VDPC model.
- Significant fluorescent iron lines (6.4 keV) are not observed.
  - Absorbers are preferential located in the line of sights

# 4. Structure around the AGN

Disk winds simulation:
outflows are limited in a narrow range of the zenith angle

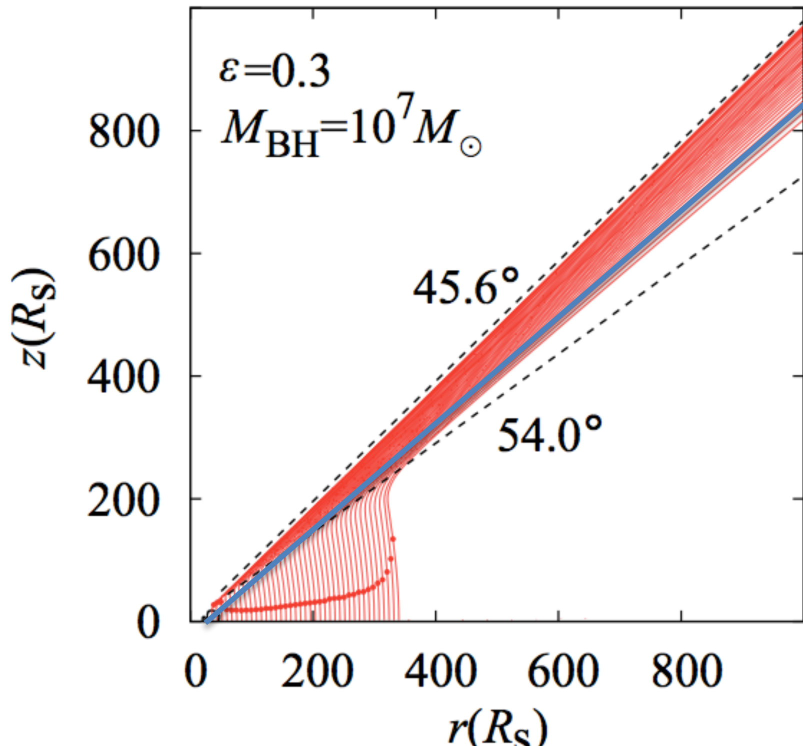


Nomura et al. (2013)

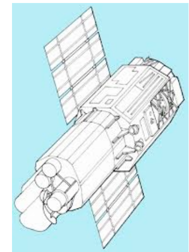

Partially
Absorbed
X-rays

Line-of-sight is aligned to the outflow?

# Contents

# Contents

# Comparison of BHB and AGN RMS spectra

- If the broad iron line production mechanism is identical in AGN and BHB, we should expect the same RMS spectra, where the timescale is normalized by BH mass.
- Studying BHB with CCD with ~msec time-resolution is only recently made possible (using Suzaku P-sum mode; Mizumoto et al. 2015)

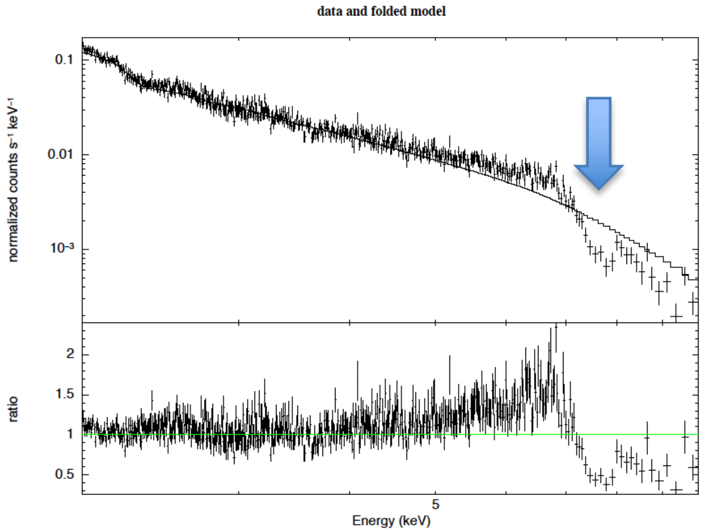


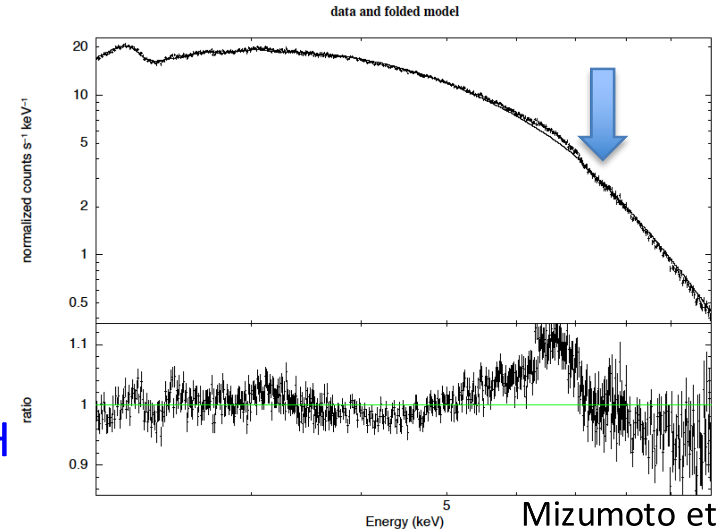


Mizumoto et al. (2015)

$10^5$ BH mass difference

1H0707+405 with Suzaku

GRS1915+105 with Suzaku

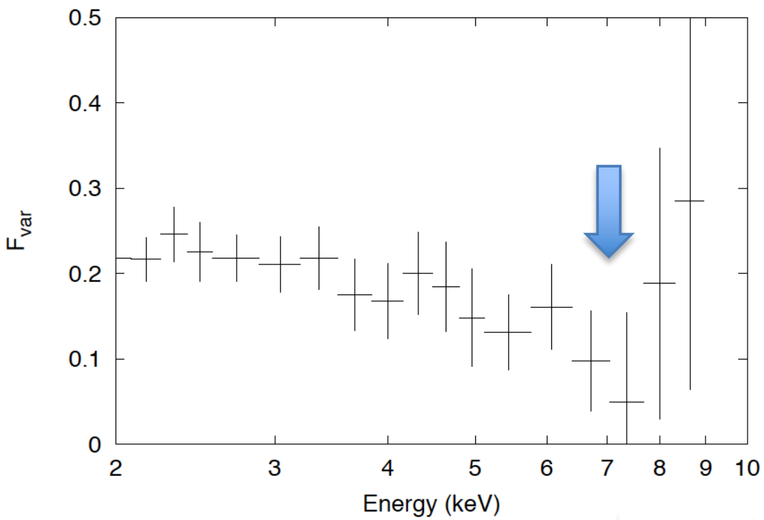


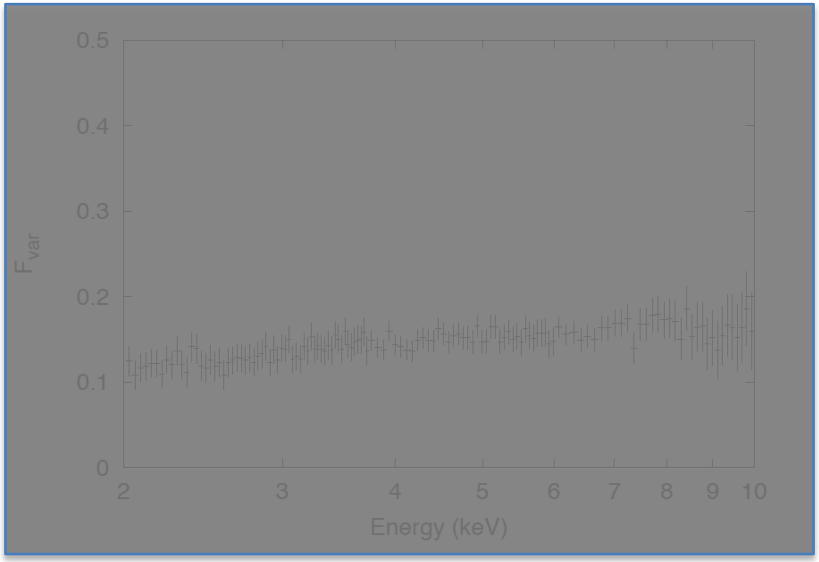


Energy Spectra of Variable Component
$\Delta$T=8000sec

Energy Spectra of Variable Component
$\Delta$T=80msec

*Broad iron line feature is NOT normalized by the black hole mass*

Mizumoto et al. (2015)

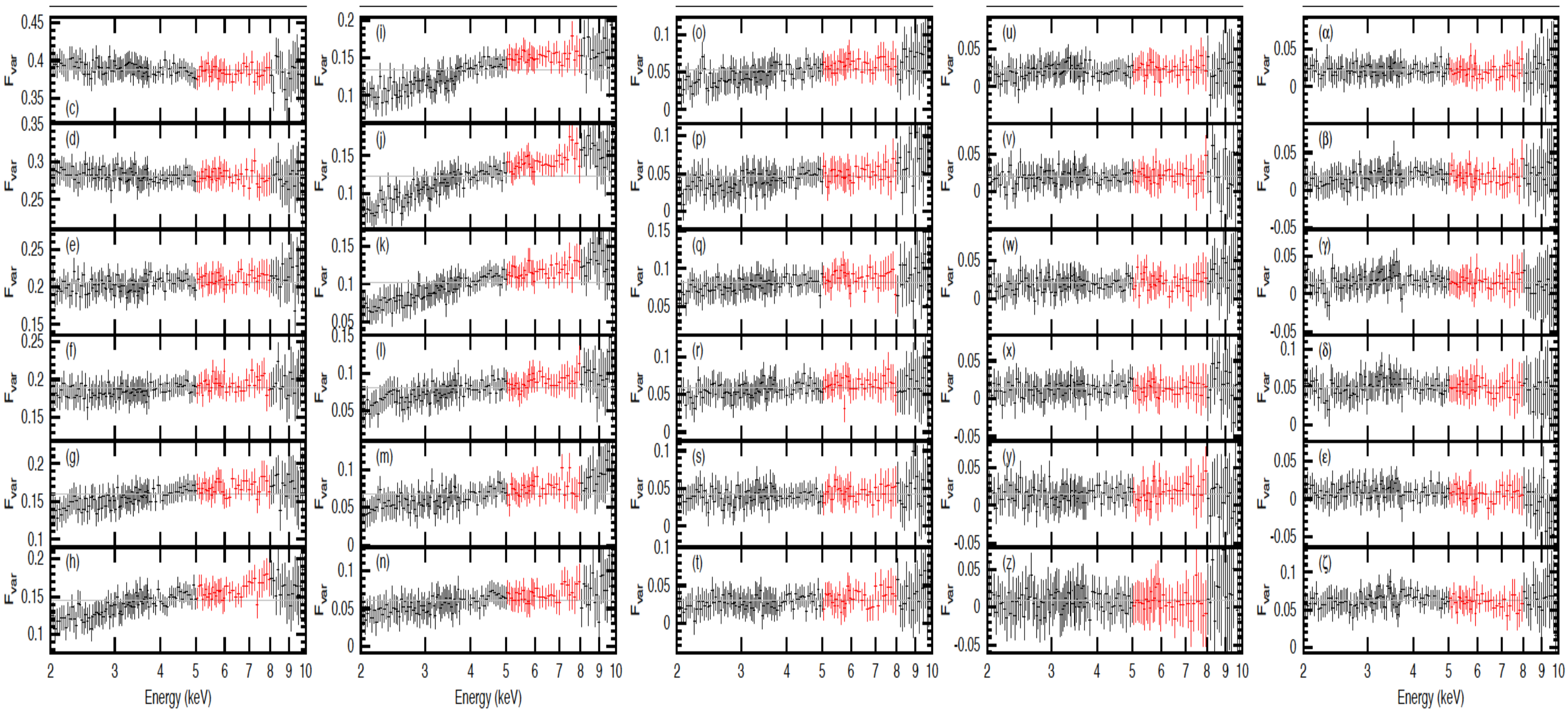


Iron line variation is not found in any time scales (ΔT=16msec~64 ksec)

# Origin of the difference between the AGN and BHB broad iron-line variation

- In principle, the X-ray luminosity variation ($t_{lum}$) and the variation of the partial absorption ($t_{abs}$) have different time scales
- In AGN, $t_{lum} >> t_{abs}$
  – Spectral variation <10 keV is caused by change of the partial absorption
- In BHB, $t_{lum} \approx t_{abs}$
  – Two independent spectral variations cancelled

# Difference of the outflow mechanisms

Mizumoto et al. (2015)

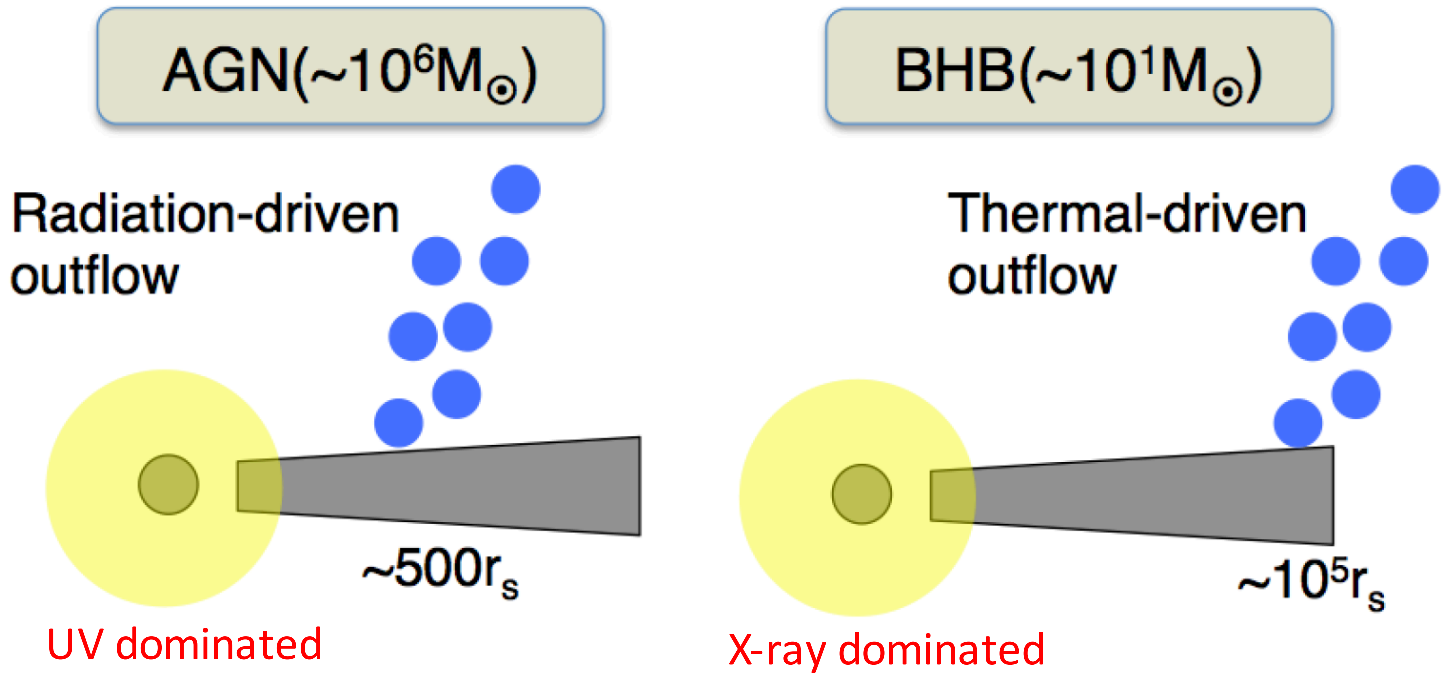


Location and timescale of the outflow are NOT normalized by BH mass

→ Origin of difference of the broad iron line variation

# Contents

# Contents

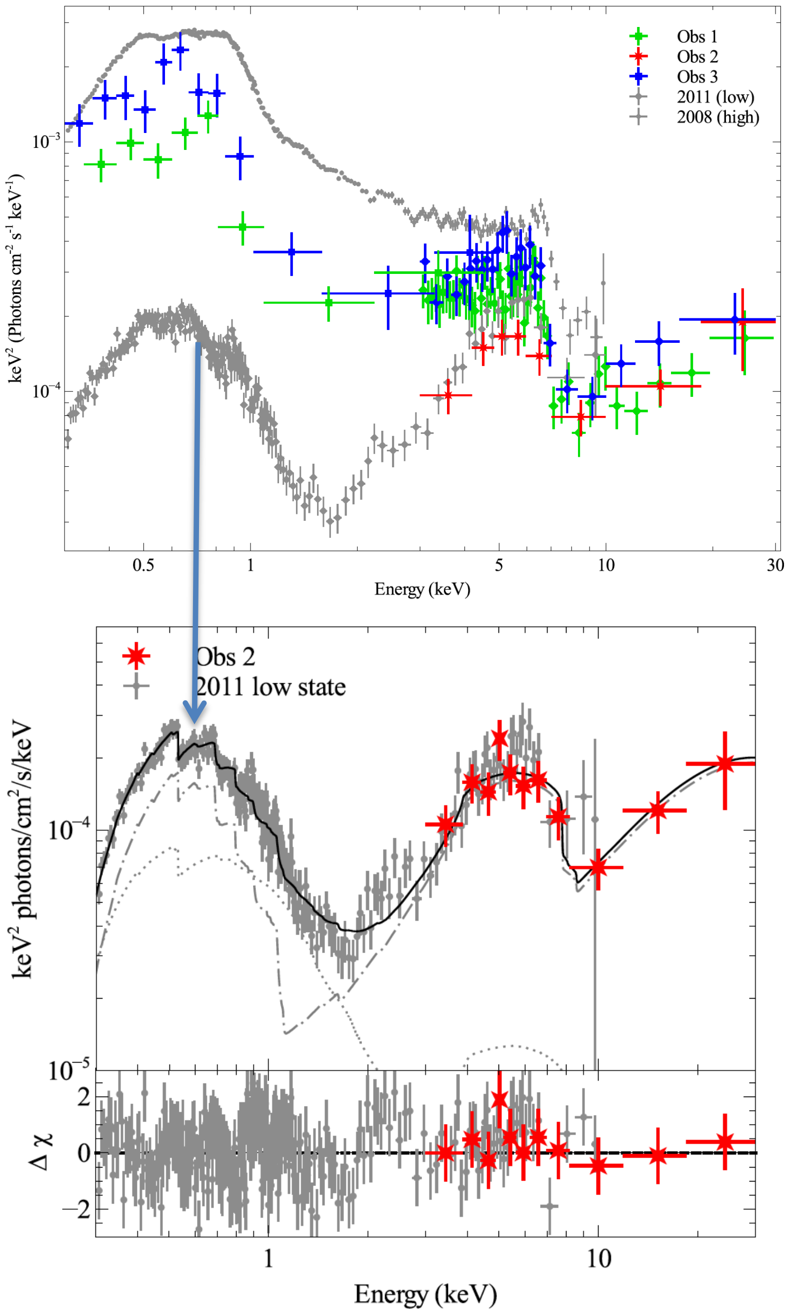


# Kara et al. (2015)
# 1H0707-495
# NuStar + XMM

Relativistic disk-line model requires an extreme condition

| Parameter | Value | |
|---|---|---|
| $N_{H(Gal)}$ $(cm^{-2})^{\alpha}$ | $5.8 \times 10^{20}$ | |
| $N_{H(int)}$ $(cm^{-2})$ | $<1 \times 10^{20}$ | No absorption |
| $h$ $(r_g)$ | $<1.4$ | Source height very low |
| $a$ | $>0.988$ | Extreme spin |
| $i$ (°) | $65.0 \pm 14.0$ | |
| $r_{out}$ $(r_g)^{\alpha}$ | 400.0 | |
| $\Gamma$ | $2.57 \pm 0.06$ | |
| $\log(\xi_1)$ $(\log(\mathrm{erg\ cm\ s^{-1}}))$ | $3.2 \pm 0.3$ | |
| $\log(\xi_2)$ $(\log(\mathrm{erg\ cm\ s^{-1}}))$ | $1.2^{+0.03}_{-0.1}$ | |
| $A_{Fe}$ | $>9.5$ | |
| $E_{cut}$ $(keV)^{\alpha}$ | 300.0 | |
| $R$ | $\gg 10$ | Direct X-rays not seen |
| $N_1 \times 10^{-7}$ | $0.1 \pm 0.4$ | |
| $N_2 \times 10^{-7}$ | $10. \pm 0.4$ | |
| $\chi^2$/dof | $403/355 = 1.14$ | |

# How can we distinguish models?

- Relativistic disk-line model requires the X-ray emission region to be very compact

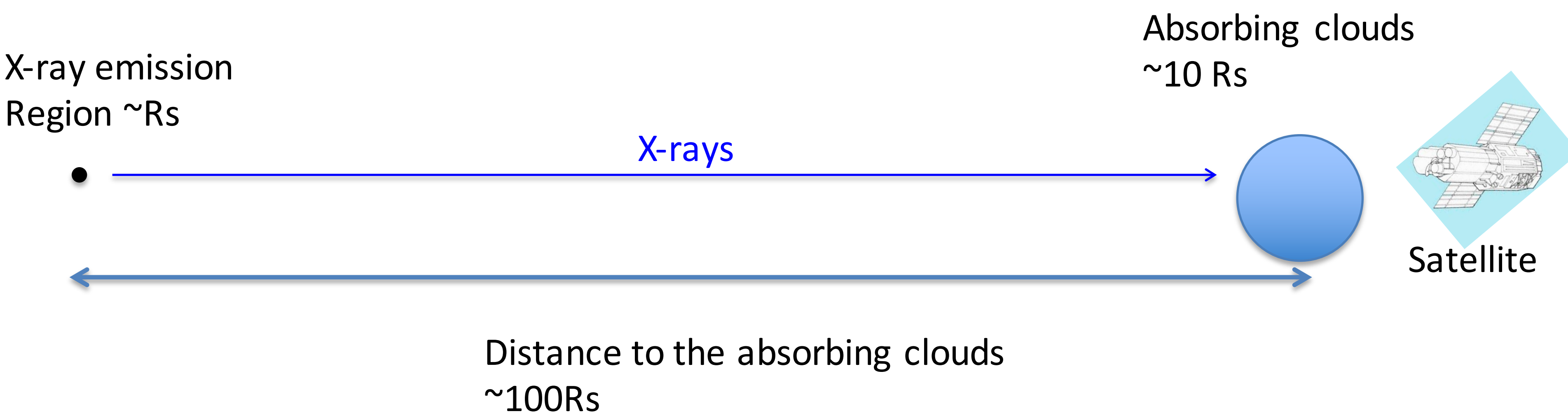


When the absorbing cloud size is larger than the X-ray source size, *partial covering does NOT take place (always full-covering)*

# How can we distinguish models?

- Partial covering model requires the X-ray emission region extended

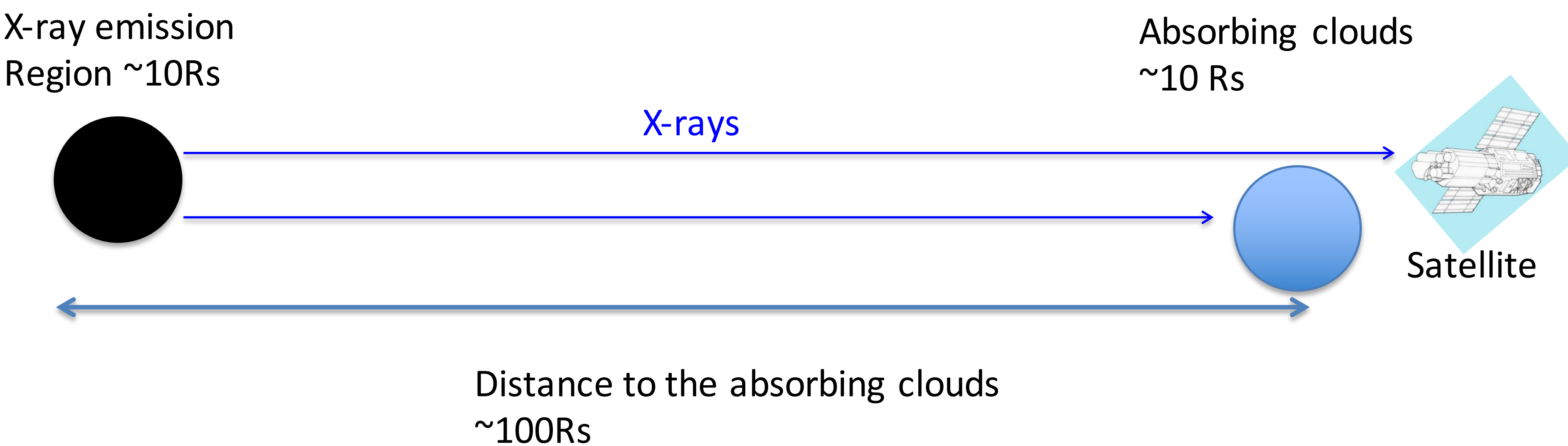


When the X-ray source size is greater than or comparative to the absorber size, *partial covering does take place*

# Evidence of partial covering in BHBs

- Superior-conjunction in Cyg X-1
  - Spectral hardening during dips

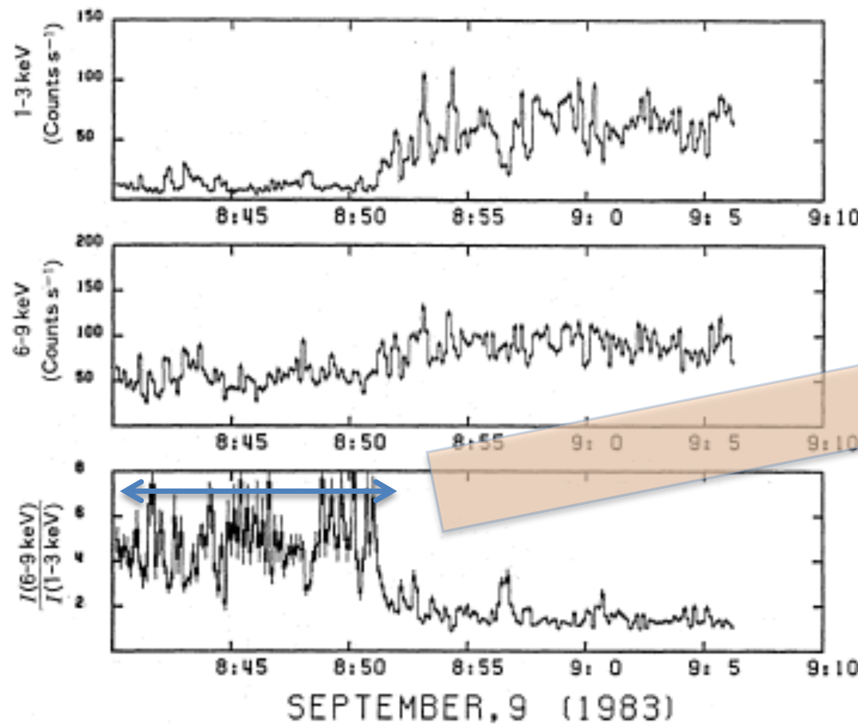


Kitamoto et al. (1985) with Tenma

Spectra during the dip period

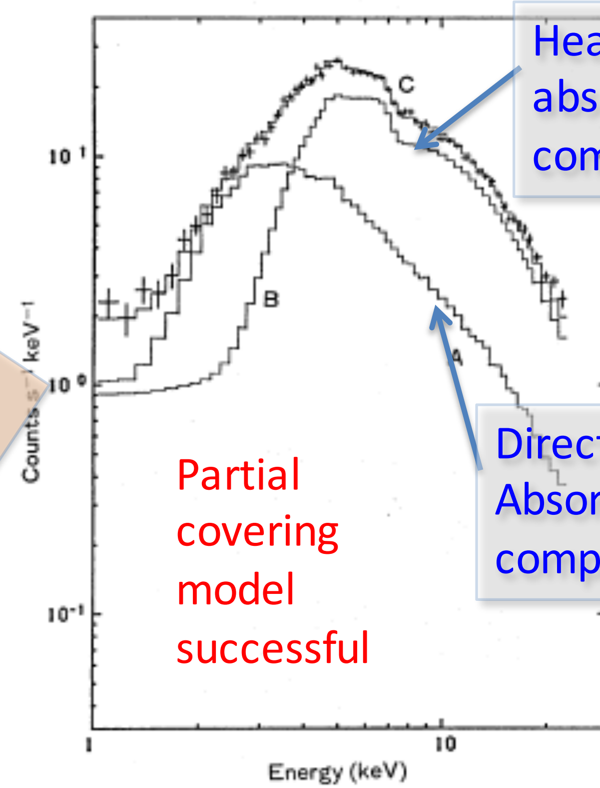


Heavily absorbed component

Direct (non-Absorbed) component

Partial covering model successful

X-ray source extended!

# How can we distinguish models?

- *Observational evidence of the partial covering*
  - *The X-ray emission region is extended*
  - *Extreme relativistic disk-line model is unlikely*

# Contents

# Contents

# 7. Conclusion

1. We analzyed X-ray energy spectra of Seyfert galaxies exhibiting seemingly broad iron line structure.
2. Partial covering phenomena are commonly observed, which indicates that the X-ray emission region is extended (~>10 Rs)
3. Observed spectral variation can be explained by the Variable Double Partial Covering Model, where the extended central X-ray source is partially covered by absorbers with two internal layers.
4. The seeming broad iron K- and L-line structures are respectively explained by the cold/thick core and the hot/thin layer of the absorbers
5. Most spectral variation is explained by independent variations of the partial covering fraction (<10 keV) and hard-tail normalization (>10 keV) .
6. The RMS spectra in 0.5-10 keV are explained by only change of the partial covering fraction.
7. The partial covering model also explains the broad iron line feature observed in the BH binary GRS1915+105
8. Variation timescales of the partial absorbers are not normalized by black hole mass